



HAL
open science

Performance Study of Two Serial Interconnected Chemostats with Mortality

Manel Dali-Youcef, Alain Rapaport, Tewfik Sari

► **To cite this version:**

Manel Dali-Youcef, Alain Rapaport, Tewfik Sari. Performance Study of Two Serial Interconnected Chemostats with Mortality. *Bulletin of Mathematical Biology*, 2022, 84 (10), 10.1007/s11538-022-01068-6 . hal-03762535

HAL Id: hal-03762535

<https://hal.inrae.fr/hal-03762535>

Submitted on 28 Aug 2022

HAL is a multi-disciplinary open access archive for the deposit and dissemination of scientific research documents, whether they are published or not. The documents may come from teaching and research institutions in France or abroad, or from public or private research centers.

L'archive ouverte pluridisciplinaire **HAL**, est destinée au dépôt et à la diffusion de documents scientifiques de niveau recherche, publiés ou non, émanant des établissements d'enseignement et de recherche français ou étrangers, des laboratoires publics ou privés.



Distributed under a Creative Commons Attribution 4.0 International License

Performance study of two serial interconnected chemostats with mortality

Manel Dali-Youcef^{1,3}, Alain Rapaport¹ and Tewfik Sari^{2*}

¹MISTEA, Univ Montpellier, INRAE, Institut Agro, Montpellier, France.

^{2*}ITAP, Univ Montpellier, INRAE, Institut Agro, Montpellier, France.

³Laboratoire de Mathématiques, Université d'Avignon, France.

*Corresponding author(s). E-mail(s): tewfik.sari@inrae.fr;

Contributing authors: daliyoucef.manel@gmail.com;

alain.rapaport@inrae.fr;

Abstract

The present work considers the model of two chemostats in series when a biomass mortality is considered in each vessel. We study the performance of the serial configuration for two different criteria which are the output substrate concentration and the biogas flow rate production, at steady state. A comparison is made with a single chemostat with the same total volume. Our techniques apply for a large class of growth functions and allow us to retrieve known results obtained when the mortality is not included in the model and the results obtained for specific growth functions in both the mathematical literature and the biological literature. In particular, we provide a complete characterization of operating conditions under which the serial configuration is more efficient than the single chemostat, i.e. the output substrate concentration of the serial configuration is smaller than that of the single chemostat or, equivalently, the biogas flow rate of the serial configuration is larger than that of the single chemostat. The study shows that the maximum biogas flow rate, relative to the dilution rate, of the series device is higher than that of the single chemostat provided that the volume of the first tank is large enough. This non-intuitive property does not occur for the model without mortality.

Keywords: chemostat, gradostat, mortality, bifurcations, global stability, operating diagram, biogas production

34

1 Introduction

35 The mathematical model of the chemostat has received a great attention in the
36 literature for many years (see for instance [16] and literature cited inside). This
37 is probably due to its relative simplicity that can explain and predict quite
38 faithfully the dynamics of real bioprocesses exploiting microbial ecosystems. It
39 is today an important tool for decision making in industrial world, such as for
40 dimensioning bioreactors or designing efficient operating conditions [13, 20].

41 Several extensions of the original model of the chemostat, considering spa-
42 tial heterogeneity, have been proposed to better cope reality (see for instance
43 [19]). Lovitt and Wimpenny has proposed the "gradostat" experimental device
44 as a collection of chemostats of same volume interconnected in series [22, 23],
45 which has led to the so-called "gradostat model" representing in a more gen-
46 eral framework a gradient of concentrations [37, 40]. The gradostat model has
47 been further generalized as the "general gradostat model" representing more
48 general interconnection graphs with tanks of different volumes [38, 39].

49 Efficient use of a chemostat in practice relies on the analysis of its per-
50 formance. The performance is considered for different criteria studied in the
51 literature [31], among which the most common are: the output substrate
52 concentration, the residence time, the biogas flow rate and the biomass pro-
53 ductivity. Particular interconnection structures have been investigated and
54 compared for the properties in terms of input-output performances (see for
55 instance [5, 7, 15, 28]). It has been notably shown that a series of reactors
56 instead of a single perfectly mixed one can significantly improve the perfor-
57 mances of the bioprocess (in terms of matter conversion) while preserving
58 the same residence time, or equivalently that the same performance can be
59 obtained with a smaller residence time considering several tanks in series
60 instead of a single one [14, 17, 24, 25, 47].

61 On another hand, it is known that in real processes, various growth con-
62 ditions can be met and that it could be difficult to setup exactly the same
63 perfect conditions in different reactors. These conditions include toxicity lev-
64 els of culture media, which means more concretely that the consideration of
65 a bacterial mortality, although often neglected compared to the removal rate,
66 might be non avoidable and could also be variable. To the best of our knowl-
67 edge, the possible impacts of mortality in the design of series of chemostats
68 has not been yet studied in the literature, which is the purpose of the present
69 work. Its contributions also cover interests in theoretical ecology for a better
70 grasp of the interplay between spatial heterogeneity and mortality in resource-
71 consumers models. Indeed, considering different removal rates in the classical
72 chemostat model or more general ones allows to consider additional mortal-
73 ity terms [21, 29, 34, 44]. However, these mathematical studies have mainly

concern analyses of equilibria and stability and not the performances of the system in presence of mortality.

In view of providing clear messages to the practitioners, we investigate how the operating diagram of a series of two interconnected chemostats in series is modified when considering different or identical mortality rates in both tanks. Operating diagrams have proven to be a good synthetic tool to summarize the possible operating modes, emphasized in [26] for its importance for bioreactors. Indeed, such diagrams are more and more often constructed both in the biological literature [26, 36, 41, 45] and the mathematical literature [1, 2, 4, 9–12, 18, 31–33, 35, 42, 43].

Then, we study the performances in terms of conversion ratio and byproduct production (such as biogas). As we shall see, several aspects are not intuitive, which show that the consideration of mortality can significantly modify the favorable operating conditions.

Along the paper, we use the abbreviations LES for locally exponentially stable and GAS for globally asymptotically stable in the positive orthant.

The paper is organized as follows. Section 2 includes the introduction of the mathematical model corresponding to the serial configuration of two chemostats with mortality rate. Afterwards, Section 3 focuses on the study of performances of the serial configuration with respect of the output substrate concentration. Then, Section 4 considers the performances of the serial configuration with respect of the biogas production. Next, Section 5 is devoted to illustrations and numerical simulations and a conclusion is given in Section 6. Moreover, we set up the single chemostat with mortality in Appendix A, while Appendix B is devoted to the existence and stability analysis of the steady states of the serial chemostat and Appendix C to its operating diagram. These results are extension of former results, in the case without mortality [7], but that have required to revisit significantly the mathematical proofs. Finally, Appendix D contains technical proofs.

2 Presentation of the model

We consider two serial interconnected chemostats where the total volume V is divided into $V_1 = rV$ and $V_2 = (1 - r)V$, with $r \in (0, 1)$, as shown in Fig. 1. The substrate and the biomass concentrations in the tank i are respectively denoted S_i and x_i , $i = 1, 2$. The input substrate concentration in the first chemostat is designated S^{in} , the flow rate is constant and is designated by Q . The output substrate concentration is the concentration of substrate in the second tank $S^{out} = S_2$.

The mathematical model is given by the following equations:

4 Performance study of two serial interconnected chemostats

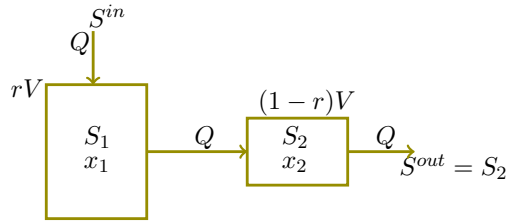


Fig. 1 The serial configuration of two chemostats respectively of volumes rV and $(1-r)V$.

$$\begin{aligned}
 \dot{S}_1 &= \frac{D}{r}(S^{in} - S_1) - f(S_1)x_1 \\
 \dot{x}_1 &= -\frac{D}{r}x_1 + f(S_1)x_1 - ax_1 \\
 \dot{S}_2 &= \frac{D}{1-r}(S_1 - S_2) - f(S_2)x_2 \\
 \dot{x}_2 &= \frac{D}{1-r}(x_1 - x_2) + f(S_2)x_2 - ax_2,
 \end{aligned} \tag{1}$$

112 where $\dot{S}_i = \frac{dS_i}{dt}$, $\dot{x}_i = \frac{dx_i}{dt}$, $i = 1, 2$, f is the growth function such that $f(S_i)$
 113 is the growth function of the substrate in the tank $i = 1, 2$, a is the mortality
 114 rate of the biomass and $D = Q/V$ is the dilution rate of the whole structure.
 115 The dilution rate of the first tank is $Q/V_1 = D/r$. The dilution rate of the
 116 second tank is $Q/V_2 = D/(1-r)$.

117 Note that these equations are not valid for $r = 0$ and $r = 1$, which corre-
 118 spond to a single chemostat. For sake of completeness, the useful results on
 119 the single chemostat are given in Appendix A. The considered growth function
 120 satisfies the following properties.

121 **Assumption 1** The function f is C^1 , with $f(0) = 0$ and $f'(S) > 0$ for all $S > 0$.

We define

$$m := \sup_{S>0} f(S), \quad (m \text{ may be } +\infty). \tag{2}$$

122 As f is increasing then the *break-even concentration* is defined by

$$\lambda(D) := f^{-1}(D) \quad \text{when } 0 \leq D < m. \tag{3}$$

123 The particular case without mortality of the biomass ($a = 0$) is studied in
 124 [7]. The results on the existence and stability of steady states of system (1) are
 125 very similar to the case without mortality. The details are given in Appendix
 126 B. The system can have up to three steady states:

- 127 • The washout steady state $E_0 = (S^{in}, 0, S^{in}, 0)$.
- 128 • The steady state $E_1 = (S^{in}, 0, \bar{S}_2, \bar{x}_2)$ of washout in the first chemostat but
 129 not in the second one.
- 130 • The steady state $E_2 = (S_1^*, x_1^*, S_2^*, x_2^*)$ of persistence of the species in both
 131 chemostats.

132 As in the case without mortality, see Table C2 in the Appendix, for any
 133 operating condition (S^{in}, D) , one and only one of the steady-states E_0 , E_1 and
 134 E_2 , is stable. It is then globally asymptotically stable (GAS).

135 The operating diagram of the system is described in Appendix C. The
 136 operating diagram has as coordinates the input substrate concentration S^{in}
 137 and the dilution rate D , and shows how the solutions of the system behave for
 138 different values of these two parameters. The regions constituting the oper-
 139 ating diagram correspond to different qualitative asymptotic behaviors. The
 140 operating diagram of system (1) is depicted in Fig. 2.

141 The aim of this work is to establish a comparison of the performance of
 142 the serial configuration with ones of the single chemostat. In the following,
 143 we compare both structures according to two different criteria; the output
 144 substrate concentration and the biogas flow rate.

145 3 Output substrate concentration

146 The output substrate concentration measures the biodegradation of the input
 147 substrate by the overall device. The reduction of the output substrate concen-
 148 tration is one of the main objectives of the biological wastewater treatment,
 149 and its minimization is often addressed in the literature, see for example [46].
 150 We assume that the serial configuration is functioning at a stable steady state.
 151 The output substrate concentration at steady state depends on the parameters
 152 D , S^{in} and r , and will be denoted $S_r^{out}(S^{in}, D)$.

153 **Proposition 1** Assume that Assumption 1 is satisfied. The output substrate con-
 154 centration at steady state of system (1) is given by

$$S_r^{out}(S^{in}, D) = \begin{cases} S^{in} & \text{if } S^{in} \leq \min\left(\lambda\left(\frac{D}{1-r} + a\right), \lambda\left(\frac{D}{r} + a\right)\right) \\ \bar{S}_2 & \text{if } \lambda\left(\frac{D}{1-r} + a\right) \leq S^{in} \leq \lambda\left(\frac{D}{r} + a\right) \\ S_2^* & \text{if } S^{in} > \lambda\left(\frac{D}{r} + a\right) \end{cases} \quad (4)$$

155 where $\bar{S}_2 = \lambda\left(\frac{D}{1-r} + a\right)$ and S_2^* is the unique solution of equation $h(S_2) = f(S_2)$.
 156 In this equation, the function h is defined by:

$$h(S_2) = \frac{D+(1-r)a}{1-r} \frac{S_1^* - S_2}{b - S_2}, \quad (5)$$

157 where $S_1^* = \lambda\left(\frac{D}{r} + a\right)$ and $b = \frac{D(S^{in} - S_1^*)}{D + ra} + S_1^*$.

158 *Proof* The output substrate concentration at steady state of system (1) is equal to
 159 S^{in} , if E_0 is the GAS steady state. It is equal to \bar{S}_2 if E_1 is the GAS steady state
 160 and to S_2^* if E_2 is GAS. According to Theorem 3 in the Appendix, E_0 is GAS if and
 161 only if

$$D \geq \max(r, 1 - r)(f(S^{in}) - a),$$

6 Performance study of two serial interconnected chemostats

162 which is equivalent to

$$S^{in} \leq \min \left(\lambda \left(\frac{D}{1-r} + a \right), \lambda \left(\frac{D}{r} + a \right) \right).$$

163 On the other hand, using Theorem 3, \bar{S}_2 depends on D and r and we have
 164 $\bar{S}_2 = \lambda \left(\frac{D}{1-r} + a \right)$. E_1 is GAS if and only if

$$r(f(S^{in}) - a) \leq D \leq (1-r)(f(S^{in}) - a),$$

165 which is equivalent to

$$\lambda \left(\frac{D}{1-r} + a \right) \leq S^{in} \leq \lambda \left(\frac{D}{r} + a \right).$$

166 Finally, using Theorem 3, we know that S_2^* depends on parameters S^{in} , D , r . It
 167 is the unique solution of equation $h(S_2) = f(S_2)$, where h is defined by (5). On the
 168 other hand E_2 is GAS if and only if the condition $D < r(f(S^{in}) - a)$ is satisfied,
 169 which is equivalent to the condition $S^{in} > \lambda \left(\frac{D}{r} + a \right)$. \square

170 Although $S_r^{out}(S^{in}, D)$ is defined only for $0 < r < 1$, we can extend it, by
 171 continuity, for $r = 0$ and $r = 1$ by

$$S_0^{out}(S^{in}, D) = S_1^{out}(S^{in}, D) = S^{out}(S^{in}, D). \quad (6)$$

172 where $S^{out}(S^{in}, D)$, which is the output substrate concentration of the single
 173 chemostat, is given by

$$S^{out}(S^{in}, D) = \begin{cases} S^{in} & \text{if } S^{in} \leq \lambda(D + a), \\ \lambda(D + a) & \text{if } S^{in} > \lambda(D + a). \end{cases} \quad (7)$$

174 For more information on $S^{out}(S^{in}, D)$, see Appendix A.

175 The proof of (6), comes from the following remarks. First, we have
 176 $\bar{S}_2(D, 0) = \lambda(D + a)$ and second, according to Lemma 9 in the Appendix, we
 177 can extend $S_2^*(S^{in}, D, r)$, by continuity, to $r = 1$, by

$$S_2^*(S^{in}, D, 1) = \lambda(D + a).$$

178 Our aim in this section is to compare S_r^{out} defined by (4) and (6) and S^{out}
 179 defined by (7).

180 3.1 The serial configuration can be more efficient than 181 the single chemostat

182 We fix r and we describe the set of operating conditions (S^{in}, D) for which

$$S_r^{out}(S^{in}, D) < S^{out}(S^{in}, D), \quad (8)$$

183 that is to say, the serial configuration with volumes rV and $(1-r)V$, is more
 184 efficient than the single chemostat of volume V . For $r \in (0, 1)$, let $g_r : [0, r(m -$
 185 $a)) \mapsto \mathbb{R}$ defined by

$$g_r(D) := \lambda \left(\frac{D}{r} + a \right) + \frac{r(D+ar)}{(1-r)(D+a)} \left(\lambda \left(\frac{D}{r} + a \right) - \lambda(D + a) \right). \quad (9)$$

186 **Lemma 1** For $r \in (0, 1)$ we have $g_r(D) > \lambda\left(\frac{D}{r} + a\right)$.

187 *Proof* As $0 < r < 1$ and λ is an increasing function then, we have $\lambda(D/r + a) >$
 188 $\lambda(D + a)$. Using (9), we have $g_r(D) > \lambda(D/r + a)$. \square

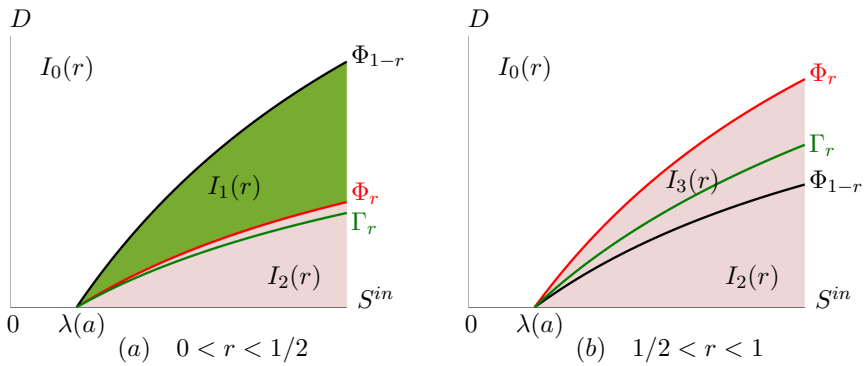


Fig. 2 The operating diagram of of system (1) and the curve Γ_r defined by (14) under which the serial configuration is more efficient than the single chemostat.

189 **Theorem 1** Assume that Assumption 1 is satisfied. For any $r \in (0, 1)$, we have

$$S_r^{out}(S^{in}, D) = S^{out}(S^{in}, D) \iff S^{in} = g_r(D).$$

190 Moreover,

$$S_r^{out}(S^{in}, D) < S^{out}(S^{in}, D) \iff S^{in} > g_r(D).$$

191 *Proof* Recall that $S_2^*(S^{in}, D, r)$ is the unique solution of equation $f(S_2) = h(S_2)$
 192 with h defined by (5). Let us first prove that

$$S_2^*(S^{in}, D, r) < \lambda(D + a) \iff S^{in} > g_r(D). \quad (10)$$

193 Since f is increasing, see Assumption 1, and h is decreasing, see Lemma 8 in the
 194 Appendix, then the condition $S_2^*(S^{in}, D, r) < \lambda(D + a)$ is equivalent to the condition
 195 $h(\lambda(D + a)) < f(\lambda(D + a)) = D + a$. Using (5), a straightforward computation shows
 196 that the condition $h(\lambda(D + a)) < D + a$ is equivalent to $S^{in} > g_r(D)$, where g_r is
 197 defined by (9). This proves (10).

198 Let us go now to the proof of the theorem. Assume that $S^{in} > g_r(D)$. Using Lemma
 199 1, we have

$$S^{in} > \lambda(D/r + a) > \lambda(D + a).$$

200 Using (4) and (7), we have

8 Performance study of two serial interconnected chemostats

$$\begin{aligned} S_r^{out}(S^{in}, D) &= S_2^*(S^{in}, D, r), \\ S^{out}(S^{in}, D) &= \lambda(D + a). \end{aligned} \quad (11)$$

From (10), we have $S_r^{out}(S^{in}, D) < S^{out}(S^{in}, D)$. Hence, we proved the following implication

$$S^{in} > g_r(D) \implies S_r^{out}(S^{in}, D) < S^{out}(S^{in}, D). \quad (12)$$

Assume now that $S^{in} \leq g_r(D)$. When $r < 1/2$, three cases must be distinguished. First, if

$$\lambda(D + a) < \lambda\left(\frac{D}{r} + a\right) < S^{in} \leq g_r(D),$$

then, by (4) and (7), we obtain (11). Hence, using (10), we have $S_r^{out}(S^{in}, D) \geq S^{out}(S^{in}, D)$. Secondly, if

$$\lambda(D + a) < \lambda\left(\frac{D}{1-r} + a\right) \leq S^{in} \leq \lambda\left(\frac{D}{r} + a\right),$$

then, by (4) and (7), we have

$$\begin{aligned} S_r^{out}(S^{in}, D) &= \lambda\left(\frac{D}{1-r} + a\right), \\ S^{out}(S^{in}, D) &= \lambda(D + a). \end{aligned}$$

Therefore, we have $S_r^{out}(S^{in}, D) > S^{out}(S^{in}, D)$. Finally, if $S^{in} \leq \lambda(D + a)$, then

$$S_r^{out}(S^{in}, D) = S^{out}(S^{in}, D) = S^{in}.$$

When $r \geq 1/2$, the proof is similar, excepted that we must distinguish only two cases, $\lambda(D + a) < S^{in} \leq \lambda(D/r + a)$ and $S^{in} \leq \lambda(D + a)$. Hence, we have proved the reciprocal implication of (12). This completes the proof of second equivalence in the theorem.

The same calculations show the equivalence if inequalities are replaced by equalities. \square

Theorem 1 asserts that the serial configuration is more efficient than the single chemostat if and only if $S^{in} > g_r(D)$. Let us illustrate this result in the operating diagram of system (1). Consider the curve of equation

$$\Phi_r = \{(S^{in}, D) : S^{in} = \lambda(D/r + a)\}. \quad (13)$$

According to the results given in Appendix C, the curves Φ_r and Φ_{1-r} defined by (13) separate the operating plane (S^{in}, D) in four regions in which the system has different asymptotic behaviour, see Table C2. To put it simply, in the $I_0(r)$ region, E_0 is GAS, in $I_1(r)$, E_1 is GAS, and in $I_2(r) \cap I_3(r)$, E_3 is GAS, see Fig. 2. This figure also shows the plot of the curve Γ_r , defined by

$$\Gamma_r := \{(S^{in}, D) : S^{in} = g_r(D)\}. \quad (14)$$

Using Lemma 1, we see that for all $r \in (0, 1)$, the curve Γ_r is always at right of the curve Φ_r . According to Theorem 1, the output substrate concentration of the serial configuration is smaller than the one of the single chemostat, if and only if (S^{in}, D) is at right of the curve Γ_r depicted in Fig. 2.

3.2 The output substrate concentration as a function of the volume fraction r

In this section we assume that (S^{in}, D) is fixed and we look at the values of r for which (8) holds. More precisely we are going to describe the function

$$r \mapsto S_r^{out}(S^{in}, D). \quad (15)$$

Proposition 2 *Assume that Assumption 1 is satisfied. Let $D > 0$, $S^{in} > \lambda(a)$. We denote $r_0 = D/(f(S^{in}) - a)$.*

1. *If $S^{in} \leq \lambda(D + a)$, then for any $r \in [0, 1]$, one has $S_r^{out}(S^{in}, D) = S^{out}(S^{in}, D) = S^{in}$.*
2. *If $\lambda(D + a) < S^{in} < \lambda(2D + a)$, then $1/2 < r_0 < 1$ and one has*

$$S_r^{out}(S^{in}, D) = \begin{cases} \bar{S}_2 & \text{if } 0 \leq r \leq 1 - r_0 \\ S^{in} & \text{if } 1 - r_0 \leq r \leq r_0 \\ S_2^* & \text{if } r_0 \leq r \leq 1. \end{cases} \quad (16)$$

3. *If $\lambda(2D + a) \leq S^{in}$, then $0 < r_0 \leq 1/2$ and one has*

$$S_r^{out}(S^{in}, D) = \begin{cases} \bar{S}_2 & \text{if } 0 \leq r \leq r_0 \\ S_2^* & \text{if } r_0 \leq r \leq 1. \end{cases} \quad (17)$$

Here $\bar{S}_2 = \lambda\left(\frac{D}{1-r} + a\right)$ and $S_2^* = S_2^*(S^{in}, D, r)$ is the unique solution of equation $f(S_2) = h(S_2)$, where h is defined by (5).

Proof If $S^{in} \leq \lambda(D + a)$, then, for all $r \in (0, 1)$, one has

$$S^{in} \leq \lambda(D + a) \leq \min\left\{\lambda\left(\frac{D}{1-r} + a\right), \lambda\left(\frac{D}{r} + a\right)\right\}.$$

Then, according to (4), one has $S_r^{out}(S^{in}, D) = S^{in}$. This proves item 1 of the proposition.

Let $r_0 = D/(f(S^{in}) - a)$, i.e. $S^{in} = \lambda(D/r_0 + a)$.

If $\lambda(D + a) < S^{in} < \lambda(2D + a)$, then $r_0 \in (1/2, 1)$, so that $1 - r_0 < r_0$. The interval $[0, 1]$ is subdivided into three sub-intervals. Firstly, if $0 \leq r \leq 1 - r_0 < r_0$, then $r < r_0 \leq 1 - r$, so that

$$\lambda\left(\frac{D}{1-r} + a\right) \leq S^{in} = \lambda\left(\frac{D}{r_0} + a\right) < \lambda\left(\frac{D}{r} + a\right).$$

Hence, according to (4), one has

$$S_r^{out}(S^{in}, D) = \lambda\left(\frac{D}{1-r} + a\right).$$

Secondly, if $1 - r_0 \leq r \leq r_0$, then $r_0 \geq \max\{r, 1 - r\}$, so that

$$S^{in} = \lambda\left(\frac{D}{r_0} + a\right) \leq \min\left\{\lambda\left(\frac{D}{1-r} + a\right), \lambda\left(\frac{D}{r} + a\right)\right\}.$$

245 Hence, according to (4), one has $S_r^{out}(S^{in}, D) = S^{in}$. Finally, if $r_0 < r \leq 1$, then one
 246 has

$$S^{in} = \lambda \left(\frac{D}{r_0} + a \right) > \lambda \left(\frac{D}{r} + a \right).$$

247 Hence, according to (4), one has

$$S_r^{out}(S^{in}, D) = S_2^*(S^{in}, D, r).$$

248 This proves item 2 of the proposition.

249 If $\lambda(2D+a) \leq S^{in}$, then $r_0 \in (0, 1/2]$. Therefore, $r_0 \leq 1 - r_0$. The proof of item 3
 250 of the proposition is the same as the proof of item 2 excepted that now, the interval
 251 $[0, 1]$ is subdivided now into two sub-intervals $[0, r_0]$ and $[r_0, 1]$, so that the interval
 252 for which $S_r^{out}(S^{in}, D) = S^{in}$ is empty. \square

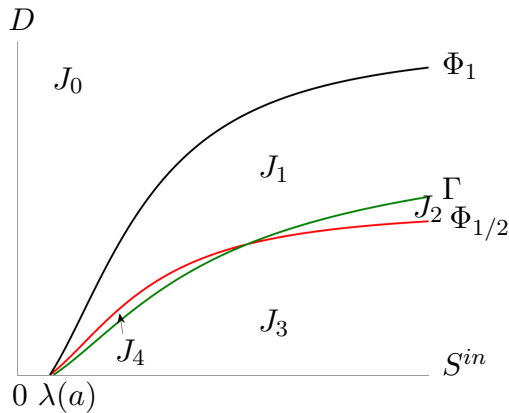


Fig. 3 In each region J_i , $i = 0, \dots, 4$, the map $r \mapsto S_r^{out}(S^{in}, D)$ for fixed (S^{in}, D) has a different behavior.

253 We want to determine the values $r \in (0, 1)$ for which the condition (8) is
 254 satisfied. We need the following Assumption that is satisfied by any concave
 255 growth function but also by non concave growth functions, satisfying additional
 256 conditions, see Section 3.4.

257 **Assumption 2** For every $D \in [0, m-a)$, the function $r \in (D/(m-a), 1) \mapsto g_r(D) \in$
 258 \mathbb{R} is decreasing.

259 Let $D < m - a$. Using $g_r(D) > \lambda(D/r + a)$, we have

$$\lim_{r \rightarrow D/(m-a)} g_r(D) > \lim_{r \rightarrow D/(m-a)} \lambda(D/r + a) = +\infty.$$

260 On the other hand, using L'Hôpital's rule, we have

$$\lim_{r \rightarrow 1} g_r(D) = g(D). \quad (18)$$

261 where $g : [0, m - a) \rightarrow \mathbb{R}^+$ is defined by

$$g(D) = \lambda(D + a) + D\lambda'(D + a). \quad (19)$$

262 Therefore, from Assumption 2, the function $r \mapsto g_r(D)$ is decreasing from
263 $(D/(m - a), 1)$ to $(g(D), +\infty)$. Hence, it admits an inverse function

$$S^{in} \in (g(D), +\infty) \mapsto r_1(S^{in}, D) \in (D/(m - a), 1).$$

264 We use the notation $r_1(\cdot, D)$ to recall the dependence of the inverse function
265 in D . For all $D \in (0, m - a)$, $r \in (D/(m - a), 1)$ and $S^{in} > g(D)$, we have

$$r = r_1(S^{in}, D) \iff S^{in} = g_r(D), \quad (20)$$

$$r > r_1(S^{in}, D) \iff S^{in} > g_r(D). \quad (21)$$

266 **Theorem 2** Assume that Assumptions 1 and 2 are satisfied. Let g defined by (19).

- 267 • If $S^{in} \leq g(D)$ then for any $r \in (0, 1)$, we have $S_r^{out}(S^{in}, D) > S^{out}(S^{in}, D)$.
- 268 In addition, for $r = 0$ and $r = 1$ we have $S_r^{out}(S^{in}, D) = S^{out}(S^{in}, D)$.
- 269 • If $S^{in} > g(D)$ then $S_r^{out}(S^{in}, D) < S^{out}(S^{in}, D)$ if and only if $r_1(S^{in}, D) <$
270 $r < 1$, with $r_1(S^{in}, D)$, defined by (20). In addition, for $r = 0$, $r =$
271 $r_1(S^{in}, D)$ and $r = 1$, we have $S_r^{out}(S^{in}, D) = S^{out}(S^{in}, D)$.

272 *Proof* The function $r \mapsto g_r(D)$ is decreasing and tends to $g(D)$ as r tends to 1, as
273 shown by (18). Thus, for all $r \in (0, 1)$, we have $g(D) < g_r(D)$. If $S^{in} \leq g(D)$, then
274 $S^{in} < g_r(D)$. According to Theorem 1, for all $r \in (0, 1)$, we have $S_r^{out}(S^{in}, D) >$
275 $S^{out}(S^{in}, D)$.

276 Let $S^{in} > g(D)$. Let $r_1 = r_1(S^{in}, D)$. According to (21), for all $r > r_1$, we have
277 $S^{in} > g_r(D)$. Thus, according to Theorem 1, we have $S_r^{out}(S^{in}, D) < S^{out}(S^{in}, D)$.

278 The equality $S_r^{out}(S^{in}, D) = S^{out}(S^{in}, D)$ is verified for the $r = 0$ and $r = 1$, see
279 (6). In addition, we have $S^{in} = g_{r_1}(D)$, see (20). Hence, according to Theorem 1, we
280 have $S_{r_1}^{out}(S^{in}, D) = S^{out}(S^{in}, D)$. \square

281 Let us now describe the subsets of the operational space (S^{in}, D) for which
282 the behaviour described in the three cases of Proposition 2 occurs. For a complete
283 description we will also distinguish the sub-cases for which there exists
284 $r_1 = r_1(S^{in}, D)$ such that, for $r_1 < r < 1$, (8) is satisfied, as shown in Theorem
285 2. Consider the curves Φ_1 and $\Phi_{1/2}$, defined by (13), and the curve Γ defined
286 by

$$\Gamma := \{(S^{in}, D) : S^{in} = g(D)\}, \quad (22)$$

287 These three curves intersect at $(\lambda(a), 0)$ and, using the inequality $g(D) >$
288 $\lambda(D + a)$, which is satisfied for all $D > 0$, one deduces that Γ is at the right

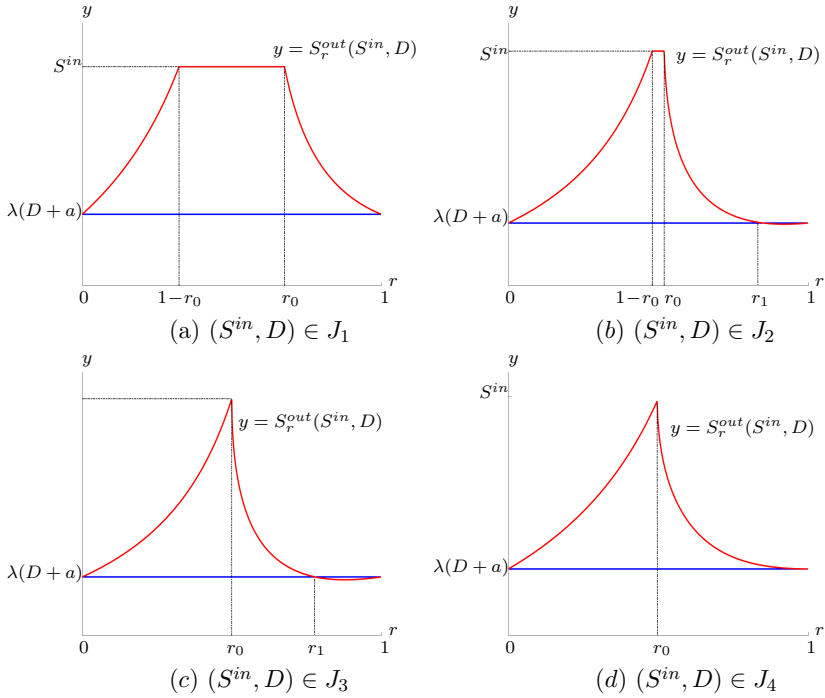


Fig. 4 For S^{in} and D fixed, the output substrate concentration of the serial configuration, in red, compared to that of the single chemostat, in blue; $r_1(S^{in}, D)$ is defined by (20), $r_0 = D/(f(S^{in}) - a)$ and J_1, J_2, J_3, J_4 are depicted in Fig. 3.

of Φ_1 . Therefore, the curves $\Phi_1, \Phi_{1/2}$ and Γ separate the set of operating parameters (S^{in}, D) into the following four subsets, see Fig. 3.

$$\begin{aligned}
 J_0 &= \{(S^{in}, D) : S^{in} \leq \lambda(2D + a)\}, \\
 J_1 &= \{(S^{in}, D) : \lambda(D + a) < S^{in} \leq \min\{g(D), \lambda(2D + a)\}\}, \\
 J_2 &= \{(S^{in}, D) : g(D) < S^{in} < \lambda(2D + a)\}, \\
 J_3 &= \{(S^{in}, D) : \max\{g(D), \lambda(2D + a)\} \leq S^{in}\}, \\
 J_4 &= \{(S^{in}, D) : \lambda(2D + a) < S^{in} < g(D)\}.
 \end{aligned} \tag{23}$$

Combining the results of Proposition 2 and Theorem 2, we find that the function $r \mapsto S_r^{out}(S^{in}, D)$ is as in Fig. 4. In the following we will comment on this figure.

- If $(S^{in}, D) \in J_1$, then when $S^{in} < \lambda(2D + a)$, $S_r^{out}(S^{in}, D)$ is given by (16) and when $S^{in} = \lambda(2D + a)$, $S_r^{out}(S^{in}, D)$ is given by (17). In addition, for all $r \in (0, 1)$, $S_r^{out}(S^{in}, D) > S^{out}(S^{in}, D)$. The equality is fulfilled for $r = 0$ and $r = 1$, see Fig. 4(a).
- If $(S^{in}, D) \in J_2$, then $S_r^{out}(S^{in}, D)$ is given by (16) and $S_r^{out}(S^{in}, D) < S^{out}(S^{in}, D)$ if and only if $r \in (r_1(S^{in}, D), 1)$, where $r_1(S^{in}, D)$ is defined

by (20). The equality is fulfilled for $r = 0$, $r = r_1(S^{in}, D)$ and $r = 1$, see Fig. 4(b).

- If $(S^{in}, D) \in J_3$ then $S_r^{out}(S^{in}, D)$ is given by (17) and $S_r^{out}(S^{in}, D) < S^{out}(S^{in}, D)$ if and only if $S^{in} > g(D)$ and $r \in (r_1(S^{in}, D), 1)$ where $r = r_1(S^{in}, D)$ is defined by (20). The equality is fulfilled for $r = 0$, $r = r_1(S^{in}, D)$ and $r = 1$, see Fig. 4(c).
- If $(S^{in}, D) \in J_4$ then $S_r^{out}(S^{in}, D)$ is given by (17) and for all $r \in (0, 1)$, $S_r^{out}(S^{in}, D) > S^{out}(S^{in}, D)$. The equality is fulfilled for $r = 0$ and $r = 1$, see Fig. 4(d).

Note that if $(S^{in}, D) \in J_0$, then case 1 of Proposition 2 occurs. One remarks that the lowest value of the red curve, corresponding to the lowest output substrate concentration of the serial configuration, is obtained for $(S^{in}, D) \in J_2 \cap J_3$ and $r > r_1(S^{in}, D)$. This lowest concentration is obtained with the best possible serial configuration.

Figures 2, 3 and 4 are made without graduations on the axes because they represent general situations where the growth function is only assumed to verify our hypotheses. It should be noticed that regions J_0 , J_1 and J_3 always exist and are connected. However, regions the J_2 and J_4 do not always exist or are necessarily connected. This depends on the number of points of intersection between curves $\Phi_{1/2}$ and Γ . For a linear growth rate, $\Phi_{1/2} = \Gamma$ and hence, regions J_2 and J_4 do not exist, see Fig. 7(a). For a Monod growth function, curves $\Phi_{1/2}$ and Γ intersect only at point $(\lambda(a), 0)$ and hence, region J_3 always exist and is connected but region J_3 does not exist, see Fig. 8(a). For a Hill growth function, curves $\Phi_{1/2}$ and Γ always intersect at $(\lambda(a), 0)$ and also at a unique positive point, Lemma 6. Hence, regions J_2 and J_4 both exist and are connected, see Fig. 9(a,b,c).

3.3 The output substrate concentration as a function of the dilution rate

In this section we assume that S^{in} and r are fixed and we look at the values of the dilution rate D for which (8) holds, i.e. the serial configuration, is more efficient than the single chemostat. More precisely we are going to describe the function

$$D \mapsto S_r^{out}(S^{in}, D). \quad (24)$$

We want to determine the subset of values of D for which the condition (8) is satisfied. We need the following Assumption that is satisfied by any concave growth function, but also by non concave growth functions, satisfying additional conditions, see Section 3.4.

Assumption 3 For every $r \in (0, 1)$, the function $D \in [0, r(m - a)) \mapsto g_r(D) \in \mathbb{R}$ is increasing.

Using $g_r(D) > \lambda(D/r + a)$, we have

$$\lim_{D \rightarrow r(m-a)} g_r(D) > \lim_{D \rightarrow r(m-a)} \lambda(D/r + a) = +\infty.$$

From Assumption 3, the function $D \mapsto g_r(D)$ is increasing from $[0, r(m-a))$ to $[g_r(0) = \lambda(a), +\infty)$. Hence, it admits an inverse function

$$S^{in} \in (\lambda(a), +\infty) \mapsto D_r(S^{in}) \in [0, r(m-a)).$$

For all $r \in (0, 1)$, $S^{in} \geq \lambda(a)$ and $D \in [0, r(m-a))$, we have

$$D = D_r(S^{in}) \iff S^{in} = g_r(D), \quad (25)$$

$$D < D_r(S^{in}) \iff S^{in} > g_r(D). \quad (26)$$

Proposition 3 *Assume that Assumptions 1 and 3 are satisfied. We have*

$$S_r^{out}(S^{in}, D) < S^{out}(S^{in}, D) \iff 0 < D < D_r(S^{in}),$$

338 where $D_r(S^{in})$ is defined by (25).

339 *Proof* Let $r \in (0, 1)$. According to (26), if $D < D_r(S^{in})$, then $S^{in} > g_r(D)$. Conse-
340 quently, according to Theorem 1, we have $S_r^{out}(S^{in}, D) < S^{out}(S^{in}, D)$. \square

341 3.4 How to check Assumptions 2 and 3

342 In this section we give sufficient conditions for Assumption 2 and 3 to be
343 satisfied. These conditions will be useful for the applications given in Section
344 5. For this purpose we consider the function γ defined by

$$\gamma(r, D) = g_r(D), \quad (27)$$

defined on

$$\text{dom}(\gamma) = \{(r, D) : 0 < r < 1, 0 < D/r + a < m\},$$

345 which consists simply in considering $g_r(D)$, given by (9), as a function of both
346 variables r and D . If

$$\frac{\partial \gamma}{\partial r}(r, D) < 0 \text{ for all } (r, D) \in \text{dom}(\gamma),$$

347 then Assumption 2 is satisfied. Similarly, if

$$\frac{\partial \gamma}{\partial D}(r, D) > 0 \text{ for all } (r, D) \in \text{dom}(\gamma),$$

348 then Assumption 3 is satisfied. The following Lemmas give sufficient condi-
349 tions, for partial derivatives of γ to have their signs as indicated above.

350 **Lemma 2** For $D \in (0, m - a)$, let l_D be defined on $\text{dom}(l_D) = (D/(m - a), 1]$ by
 351 $l_D(r) = \lambda(D/r + a)$.

a) Assume that for $D \in (0, m - a)$ and $r \in \text{dom}(l_D)$ we have

$$l_D(1) > l_D(r) + (1 - r)l'_D(r) \quad (28)$$

352 then, for all $(r, D) \in \text{dom}(\gamma)$, we have $\frac{\partial \gamma}{\partial r}(r, D) < 0$.

353 b) If, for $D \in (0, m - a)$, l_D is strictly convex on $\text{dom}(l_D)$, then the condition (28)
 354 is satisfied.

355 c) If f is twice derivable, then l_D is twice derivable and the following conditions are
 356 equivalent

- 357 1. For $D \in (0, m - a)$ and $r \in \text{dom}(l_D)$, $l''_D(r) > 0$.
- 358 2. For $S > \lambda(a)$, $(f(S) - a)f''(S) < 2(f'(S))^2$.

Proof Notice first that $\gamma(r, D)$ can be written as follows

$$\begin{aligned} \gamma(r, D) &= g_r(D) = \lambda(D + a) + \\ &\quad \left(\frac{1}{1-r} - \frac{ra}{D+a} \right) \left(\lambda \left(\frac{D}{r} + a \right) - \lambda(D + a) \right). \end{aligned} \quad (29)$$

Using the definition of l_D , $\gamma(r, D)$ is given then by

$$\gamma(r, D) = l_D(1) + \left(\frac{1}{1-r} - \frac{ra}{D+a} \right) (l_D(r) - l_D(1)).$$

359 The partial derivative, with respect to r of γ is given then by

$$\begin{aligned} \frac{\partial \gamma}{\partial r}(r, D) &= \frac{a(1-2r)}{D+a} l'_D(r) + \\ &\quad \left(\frac{1}{(1-r)^2} - \frac{a}{D+a} \right) (l_D(r) - l_D(1) + (1-r)l'_D(r)). \end{aligned} \quad (30)$$

Notice that $\frac{1}{(1-r)^2} - \frac{a}{D+a} > 0$ for all $r \in (0, 1)$. From $l'_D(r) = -\frac{D}{r^2} \lambda' \left(\frac{D}{r} + a \right)$, it is deduced that $l'_D(r) < 0$. Therefore, if the condition (28) is satisfied, and, in addition $0 < r \leq 1/2$, then, from (30), it is deduced that $\frac{\partial \gamma}{\partial r}(r, D) < 0$.

In the case $r \in (1/2, 1)$, we use the following expression of $\gamma(r, D)$ which is deduced from (29):

$$\gamma(r, D) = l_D(1) + B(r) \frac{l_D(r) - l_D(1)}{1-r},$$

where $B(r) = \frac{D+a-ar(1-r)}{D+a}$. Straightforward computation show that

$$\frac{\partial \gamma}{\partial r}(r, D) = \frac{D+ar(2-r)}{(D+a)(1-r)^2} (l_D(r) - l_D(1) + (1-r)C(r)l'_D(r)), \quad (31)$$

where $C(r) = \frac{D+a-ar(1-r)}{D+ar(2-r)}$. We have

$$C'(r) = \frac{a}{(D+ar(2-r))^2} (ar^2 + 2(a + 2D)r - 3D - 2a).$$

360 Thus $C'(r) = 0$ for

$$r = r^* := \frac{1}{a} \left(\sqrt{3a^2 + 7aD + 4D^2} - a - 2D \right) \in (1/2, 1)$$

and $(r - r^*)C'(r) > 0$ for $r \in (1/2, 1)$, $r \neq r^*$. Hence, from $C(1/2) = C(1) = 1$, we have $0 < C(r) < 1$ for all $r \in (1/2, 1)$. Now, if we assume that (28) is satisfied, for $1/2 < r < 1$ we have

$$l_D(1) > l_D(r) + (1 - r)l'_D(r) > l_D(r) + (1 - r)C(r)l'_D(r).$$

361 Hence, from (31), it is deduced that $\frac{\partial \gamma}{\partial r}(r, D) < 0$. This proves part *a* of the lemma.

Moreover, if l_D is strictly convex on $\text{dom}(l_D)$ then for all s and r in $(D/(m-a), 1]$, if $s \neq r$, then

$$l_D(s) > l_D(r) + (s - r)l'_D(r).$$

Taking $s = 1$ and $r \in \text{dom}(l_D)$ one obtains the condition (28). This proves part *b* of the lemma. Assume now that f , and hence l_D , are twice derivable. Using

$$\lambda'(D) = \frac{1}{f'(\lambda(D))}, \quad \lambda''(D) = -\frac{f''(\lambda(D))}{(f'(\lambda(D)))^3}, \quad (32)$$

we can write

$$\begin{aligned} l''_D(r) &= \frac{2D}{r^3} \lambda' \left(\frac{D}{r} + a \right) + \frac{D^2}{r^4} \lambda'' \left(\frac{D}{r} + a \right) \\ &= \frac{D \left(2 \left(f' \left(\lambda \left(\frac{D}{r} + a \right) \right) \right)^2 - \frac{D}{r} f'' \left(\lambda \left(\frac{D}{r} + a \right) \right) \right)}{r^3 \left(f' \left(\lambda \left(\frac{D}{r} + a \right) \right) \right)^3}. \end{aligned}$$

362 Therefore, the condition 1 in item *c* in the lemma is equivalent to the following
363 condition: For all $D \in (0, m - a)$ and $r \in (D/(m - a), 1]$, we have

$$\frac{D}{r} f'' \left(\lambda \left(\frac{D}{r} + a \right) \right) < 2 f' \left(\lambda \left(\frac{D}{r} + a \right) \right)^2. \quad (33)$$

364 Using the notation $S = \lambda \left(\frac{D}{r} + a \right)$, which is the same as $D/r = f(S) - a$, the
365 condition (33) is equivalent to : For all $S > 0$, $(f(S) - a)f''(S) < 2(f'(S))^2$, which
366 is the condition 2 in *c* in the lemma. \square

367 **Lemma 3** Assume that

$$f' \left(\lambda \left(\frac{D}{r} + a \right) \right) \leq \frac{1}{r} f'(\lambda(D + a)). \quad (34)$$

368 Then, $\frac{\partial \gamma}{\partial D}(r, D) > 0$. Hence Assumption 3 is satisfied. If f' is decreasing, then the
369 condition (34) is satisfied.

370 *Proof* From (29) we deduce that

$$\begin{aligned} \frac{\partial \gamma}{\partial D}(r, D) &= \lambda'(D + a) + \frac{ra}{(D+a)^2} \left(\lambda \left(\frac{D}{r} + a \right) - \lambda(D + a) \right) \\ &\quad + \left(\frac{1}{1-r} - \frac{ra}{D+a} \right) \left(\frac{1}{r} \lambda' \left(\frac{D}{r} + a \right) - \lambda'(D + a) \right). \end{aligned}$$

371 Notice that $\frac{1}{1-r} - \frac{ra}{D+a} > 0$, $\lambda'(D + a) > 0$ and $\lambda \left(\frac{D}{r} + a \right) > \lambda(D + a)$. Therefore
372 the condition

$$\frac{1}{r} \lambda' \left(\frac{D}{r} + a \right) - \lambda'(D + a) \geq 0$$

373 is sufficient to have $\frac{\partial \gamma}{\partial D}(r, D) > 0$. Using (32), this condition is equivalent to (34).
374 Note that if f' is decreasing, then this condition is satisfied. Indeed, we have

$$f' \left(\lambda \left(\frac{D}{r} + a \right) \right) \leq f'(\lambda(D + a)) \leq \frac{1}{r} f'(\lambda(D + a)),$$

375 which is the condition (34). \square

376 *Remark 1* Notice that:

377 *i)* The condition 2 in part c of Lemma 2 is equivalent to the condition

$$\text{For all } S > \lambda(a), \frac{d^2}{dS^2} \left(\frac{1}{f(S)-a} \right) > 0. \quad (35)$$

378 Therefore, if f satisfies the condition (35), then it verifies Assumption 2.

379 *ii)* If the increasing growth function f is twice derivable and satisfies $f''(S) \leq 0$ for
380 all $S > 0$, then the condition b in Lemma 2 and the condition (34) in Lemma 3
381 are satisfied. Thus, Assumptions 2 and 3 are satisfied and our results apply for any
382 concave growth function.

383 *iii)* Assume that the increasing growth function f is twice derivable and there exists
384 $\hat{S} \in (0, +\infty)$ such that f'' is nonnegative on $(0, \hat{S})$ and nonpositive on $(\hat{S}, +\infty)$.
385 If moreover the condition 2 in part c of Lemma 2 is verified for $a = 0$, then this
386 condition is also verified for any $a > 0$ and $S \in (\lambda(a), \hat{S})$. Therefore, if $(1/f)'' > 0$
387 on $(0, \hat{S})$ then Assumption 2 is satisfied.

388 We will see in Section 5, how to use Remark 1 and Lemmas 2 and 3 to show
389 that a linear growth function, a Monod function and a Hill function satisfy
390 Assumptions 2 and 3.

391 4 Biogas flow rate

392 Microbial activity often produces by-products such as biogas, which can be
393 a valuable source of energy in certain contexts. For instance, the anaerobic
394 digestion of organic matter by microbial species produces methane and carbon
395 dioxide. Valorizing biogas production while treating wastewater has received
396 recently great attention, as a way of producing valuable energy and limiting
397 the carbon footprint of the process [30].

398 We recall that the biogas flow rate is proportional to the microbial activity,
399 as defined for instance in [3, 27]. We consider here the biogas flow rate as a
400 function of the input substrate concentration S^{in} , the dilution rate D and the
401 parameter r .

402 For $r(f(S^{in}) - a) \leq D < (1 - r)(f(S^{in}) - a)$, the biogas flow rate
403 corresponding to the steady state E_1 is given by the expression

$$G_1(S^{in}, D, r) = V_2 \bar{x}_2 f(\bar{S}_2), \quad (36)$$

404 with $V_2 = (1 - r)V$, \bar{x}_2 and \bar{S}_2 defined in (B15).

405 For $D < r(f(S^{in}) - a)$, the biogas flow rate corresponding to the positive
406 steady state E_2 is given by the expression

$$G_2(S^{in}, D, r) = V_1 x_1^* f(S_1^*) + V_2 x_2^* f(S_2^*), \quad (37)$$

407 with $V_1 = rV$, $V_2 = (1 - r)V$, x_1^* and S_1^* defined in (B17), x_2^* defined by (B18)
408 and S_2^* the unique solution of $h(S_2) = f(S_2)$.

Proposition 4 1. When $r(f(S^{in}) - a) \leq D$ and $D < (1 - r)(f(S^{in}) - a)$ then

$$G_1(S^{in}, D, r) = VD(S^{in} - \bar{S}_2). \quad (38)$$

2. When $D < r(f(S^{in}) - a)$ then

$$G_2(S^{in}, D, r) = VD(S^{in} - S_2^*). \quad (39)$$

Proof From system (B10), considering equation $\dot{S}_2 = 0$, one obtains $\bar{x}_2 f(\bar{S}_2) = D(S^{in} - \bar{S}_2)/(1 - r)$. Thus,

$$G_1(S^{in}, D, r) = V_1 \frac{D}{r} (S^{in} - \bar{S}_2) = VD(S^{in} - \bar{S}_2).$$

From system (B10), considering $\dot{S}_1 = 0$ and $\dot{S}_2 = 0$ gives respectively $x_1^* f(S_1^*) = D(S^{in} - S_1^*)/r$ and $x_2^* f(S_2^*) = D(S_1^* - S_2^*)/(1 - r)$. Thus, one has

$$\begin{aligned} G_2(S^{in}, D, r) &= V_1 \frac{D}{r} (S^{in} - S_1^*) + V_2 \frac{D}{1-r} (S_1^* - S_2^*) \\ &= VD(S^{in} - S_2^*). \end{aligned}$$

409 This ends the proof of the proposition. □

410 Although $G_1(S^{in}, D, r)$ and $G_2(S^{in}, D, r)$, given by (36) and (37), respectively, are not defined for $r = 0$ or $r = 1$, the formulas (38) and (39) allow them
411 to be extended to $r = 0$ and $r = 1$, as was done for S_r^{out} in (6). We can write
412

$$G_1(S^{in}, D, 0) = G_2(S^{in}, D, 1) = G_{chem}(S^{in}, D),$$

where

$$G_{chem}(S^{in}, D) = VD(S^{in} - \lambda(D + a)), \quad (40)$$

413 represents the biogas flow rate of the single chemostat when $0 < D < f(S^{in}) -$
414 a . For more information on $G_{chem}(S^{in}, D)$, see (A7) in Appendix A.

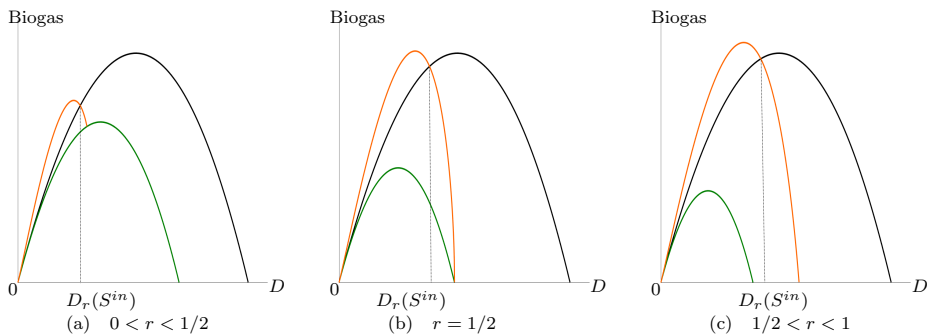


Fig. 5 For r and S^{in} fixed, the curves of the maps $D \mapsto G_1(S^{in}, D, r)$, in green, $D \mapsto G_2(S^{in}, D, r)$, in orange, and $D \mapsto G_{chem}(S^{in}, D)$, in black, where G_1 , G_2 and G_{chem} are given by (38), (39) and (40) respectively.

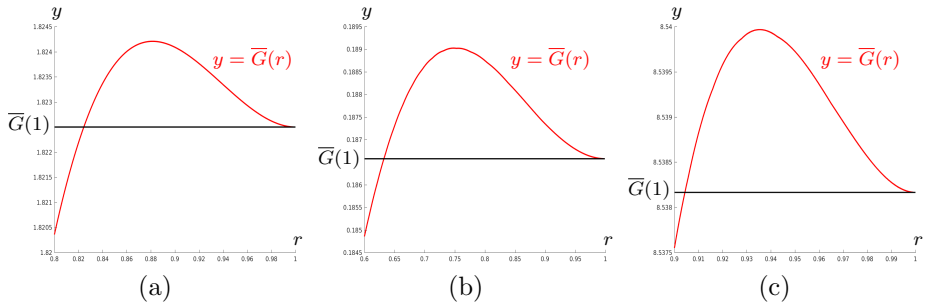


Fig. 6 The map $r \mapsto \overline{G}(r)$ with \overline{G} defined by (42). (a) $f(S) = 4S$, $a = 0.6$ and $S^{in} = 1.5$. (b) $f(S) = 4S/(5 + S)$, $a = 0.3$ and $S^{in} = 1.5$. (c) $f(S) = 4S^2/(25 + S^2)$, $a = 0.3$ and $S^{in} = 10$.

4.1 The serial configuration can be more efficient than the single chemostat

In this section, we prove that the biogas flow rate G_1 corresponding to the steady state E_1 is always smaller than the biogas flow rate of the single chemostat. However, the biogas flow rate G_2 corresponding to the steady state E_2 can be larger than the biogas flow rate of the single chemostat. More precisely, we have the following result.

Proposition 5 Assume that Assumption 1 is satisfied. Let $r \in (0, 1)$, $0 \leq D < f(S^{in}) - a$ and G_{chem} defined by (40).

1. If $r(f(S^{in}) - a) \leq D$ and $D < (1 - r)(f(S^{in}) - a)$, then $G_1(S^{in}, D, r) < G_{chem}(S^{in}, D)$, where G_1 is given by (38).
2. If $D < r(f(S^{in}) - a)$, then

$$G_2(S^{in}, D, r) > G_{chem}(S^{in}, D) \iff S^{in} > g_r(D),$$

where G_2 is given by (39) and g_r is defined by (9).

- If, in addition, Assumption 2 is satisfied, and $S^{in} > g(D)$, then $G_2(S^{in}, D, r) > G_{chem}(S^{in}, D)$, if and only if $r > r_1(S^{in}, D)$, where $r_1(S^{in}, D)$ is defined by (20).
- If, in addition, Assumption 3 is satisfied, then $G_2(S^{in}, D, r) > G_{chem}(S^{in}, D)$, if and only if $D < D_r(S^{in})$, where $D_r(S^{in})$ is defined by (25).

Proof 1. Since $D/(1 - r) > D$ and λ is increasing, we have $\lambda(D/(1 - r) + a) > \lambda(D + a)$. Then, using the formula for G_1 given in Proposition 4, this induces the inequality $G_1(S^{in}, D, r) < G_{chem}(S^{in}, D)$.

436 2. According to Theorem 1, for any $r \in (0, 1)$ and $D < r(f(S^{in}) - a)$ one
 437 has $S_2^*(S^{in}, D, r) < \lambda(D + a)$ if and only if $S^{in} > g_r(D)$. Consequently,
 438 using the formula for G_2 given in Proposition 4, one has $G_2(S^{in}, D, r) >$
 439 $G_{chem}(S^{in}, D)$ if and only if $S^{in} > g_r(D)$. If Assumption 2 is satisfied,
 440 then, using (21), we see that $G_2(S^{in}, D, r) > G_{chem}(S^{in}, D)$ if and only if
 441 $r > r_1(S^{in}, D)$. If Assumption 3 is satisfied, then, using (26), we see that
 442 $G_2(S^{in}, D, r) > G_{chem}(S^{in}, D)$ if and only if $D < D_r(S^{in})$.
 443 This ends the proof of the proposition. \square

444 Let S^{in} and D be fixed. The graphs of the biogas flow rates functions

$$r \mapsto G_1(S^{in}, D, r), \text{ and } r \mapsto G_2(S^{in}, D, r),$$

445 are easily obtained from the graph of the output substrate concentration, $r \mapsto$
 446 $S_r^{out}(S^{in}, D)$, see Fig. 4. Indeed, the formulas given in Proposition 4 show that,
 447 whenever these functions are defined, we have

$$\begin{aligned} G_1(S^{in}, D, r) &= VD(S^{in} - S_r^{out}(S^{in}, D)), \\ G_2(S^{in}, D, r) &= VD(S^{in} - S_r^{out}(S^{in}, D)). \end{aligned}$$

448 We will see in Section 5, some illustrative plots of the biogas flow rates G_1
 449 and G_2 as functions of the parameter $r \in [0, 1]$, for linear growth, see Fig. 7,
 450 Monod growth, see Fig. 8 and Hill growth, see Fig. 9.

451 Let us illustrate the result of Proposition 5 by plotting the graphs of the
 452 biogas flow rates

$$D \mapsto G_1(S^{in}, D, r) \text{ and } D \mapsto G_2(S^{in}, D, r),$$

453 when r and S^{in} are fixed, see Fig. 5. This figure is made without graduations on
 454 the axes because it represents a general situation where the growth function is
 455 only assumed to verify our hypotheses. Indeed the behaviors of the functions,
 456 depicted in this figure, follow from our results and are not simply numerical
 457 illustrations.

458 Notice that for any $r \in (0, 1)$, the graph of G_1 (plotted in green in the
 459 figure) is always below the graph G_{chem} (plotted in black). This illustrates
 460 item 1 of Proposition 5. Assuming that Assumption 3 is satisfied, then for all
 461 $0 < D < D_r(S^{in})$, the graph of G_2 (plotted in orange) is above the graph of
 462 G_{chem} (plotted in black). This illustrates item 2 of Proposition 5.

463 4.2 The maximal biogas of the serial configuration can 464 exceed that of the single chemostat

In Figure 5(c) the plot shows that the maximum of G_2 (the red curve) is larger
 than the maximum of G_{chem} , as we want to emphasize that the following
 inequality is possible

$$\max_D G_2(S^{in}, D, r) > \max_D G_{chem}(S^{in}, D). \quad (41)$$

Indeed we will show that there is a value $r^* \in (0, 1)$ such that this inequality is true for all $r \in (r^*, 1)$. The threshold r^* obviously depends on S^{in} and the rate of mortality a . It will be noted $r^*(S^{in}, a)$ when we want to highlight this dependence. This phenomenon never occurs in the case of no mortality, since we have $r^*(S^{in}, 0) = 1$. Indeed, in the case without mortality, we proved, see Proposition 6 of [7], that for all $S^{in} > 0$, and all $r \in (0, 1)$ we have

$$\max_D G_2(S^{in}, D, r) < \max_D G_{chem}(S^{in}, D),$$

465 that is to say, the maximal biogas flow rate of the serial configuration never
466 exceed the maximal biogas flow rate of the single chemostat.

467 Let us prove that, when $a > 0$, the inequality (41) is always true for r
468 sufficiently close to 1. Observe that for any fixed $S^{in} > \lambda(a)$ and $r \in (0, 1]$,
469 the continuous function $D \mapsto G_2(S^{in}, D, r)$ is defined on the closed interval
470 $[0, r(f(S^{in}) - a)]$. It is null at the extremities of this interval and positive on
471 the open interval $(0, r(f(S^{in}) - a))$. Therefore, it reaches its maximum. For a
472 given $S^{in} > \lambda(a)$, we then consider the function

$$\bar{G}(r) := \max_{D \in [0, r(f(S^{in}) - a)]} G_2(S^{in}, D, r). \quad (42)$$

473 We want to ensure that this maximum is reached at a single value, denoted
474 $\bar{D}(r)$. Note that $\bar{D}(1)$ represents the value, which we will assume to be unique,
475 at which the function $D \mapsto G_{chem}(S^{in}, D)$ reaches its maximum. We need the
476 following assumption.

477 **Assumption 4** The function f is C^2 and increasing and, for $S^{in} > \lambda(a)$, there
478 exists $\bar{D}(1) \in (0, f(S^{in}) - a)$ such that $D \mapsto G_{chem}(S^{in}, D)$ is

- 479 • strictly concave at $\bar{D}(1)$,
- 480 • increasing on $(0, \bar{D}(1))$,
- 481 • decreasing on $(\bar{D}(1), f(S^{in}) - a)$,

482 These conditions are related to the single chemostat model. They are ver-
483 ified for linear, Monod, or Hill growth functions, see Remark 3 in Appendix
484 A.

485 If Assumption 4 is satisfied, then the maximum of the function $D \mapsto$
486 $G_{chem}(S^{in}, D)$ is unique. The following lemma shows that the function $D \mapsto$
487 $G_2(S^{in}, D, r)$ satisfies the same property for r sufficiently close to 1.

488 **Lemma 4** Assume that Assumption 4 is satisfied, then for any $S^{in} > \lambda(a)$, there
489 exists a neighborhood \mathcal{V}_1 of 1, such that for any $r \in \mathcal{V}_1 \cap \{r \leq 1\}$, the maximum of
490 the function $D \mapsto G_2(S^{in}, D, r)$ is unique. We denote it by $\bar{D}(r)$. Moreover, \bar{D} is
491 differentiable on $\mathcal{V}_1 \cap \{r < 1\}$ with bounded derivative.

492 *Proof* The proof is given in in Appendix D.2. □

Proposition 6 Under Assumption 4, the function \overline{G} admits left limits of its first and second derivatives at $r = 1$, which are

$$\overline{G}'(1^-) = 0, \quad \overline{G}''(1^-) = \frac{2a\overline{D}(1)}{\overline{D}(1) + a} (S^{in} - \lambda(\overline{D}(1) + a)). \quad (43)$$

493 *Proof* The proof is given in Appendix D.3. □

Proposition 7 Under Assumption 4, there exists r^* in $(0, 1)$ such that (41) is true for any $r \in (r^*, 1)$ and

$$\max_D G_2(S^{in}, D, r^*) = \max_D G_{chem}(S^{in}, D).$$

Proof From Proposition 6, there exist $\varepsilon > 0$ such that for all $r \in (1 - \varepsilon, 1)$, we have $\overline{G}(r) > \overline{G}(1)$. Therefore, the subset I of $(0, 1)$ defined by

$$I = \{\rho \in (0, 1) : \forall r \in (\rho, 1), \overline{G}(r) > \overline{G}(1)\},$$

494 is non empty. Let r^* be the lower bound of I . We have $\overline{G}(r^*) = \overline{G}(1)$ and $\overline{G}(r) > \overline{G}(1)$
 495 for $r \in (r^*, 1)$. Using (42), we deduce that the equality in the proposition is true and
 496 (41) is true for any $r \in (r^*, 1)$. □

The function $r \mapsto \overline{G}(r)$ reaches its maximum at some $r^{max} \in (r^*, 1)$. Let $D^{max} = \overline{D}(r^{max})$ be the maximum of the function $D \mapsto G_2(S^{in}, D, r^{max})$. Therefore the maximal biogas flow rate of the serial chemostat is given by $G_2(S^{in}, D^{max}, r^{max})$. It satisfies

$$G_2(S^{in}, D^{max}, r^{max}) > G_{chem}(S^{in}, \overline{D}(1)).$$

497 We have plotted the function $r \mapsto \overline{G}(r)$ for the linear, Monod, and Hill
 498 growth functions considered in Fig. 6. It is seen in this figure that the tangent
 499 at $r = 1$ is horizontal which corresponds to $\overline{G}'(1) = 0$. In addition, one remarks
 500 that $\overline{G}(r) > \overline{G}(1)$ for r in some interval $(r^*, 1)$ and $\overline{G}(r^*) = \overline{G}(1)$. Thus,
 501 with presence of mortality rate, if practitioners are able to choose the dilution
 502 rate D , the good strategy consists in working with a serial configuration and
 503 choose r in the interval $(r^*, 1)$. The serial configuration should be operated at
 504 $D = \overline{D}(r)$, where $\overline{D}(r)$ is defined in Lemma 4.

505 *Remark 2* • If one is interested in increasing the flow of biogas, the best choice
 506 is $r = r^{max}$, $D = D^{max}$.

507 • If one is interested in reducing the dilution rate, the best choice is $r = r^*$
 508 and $D = D^*$, where $D^* = \overline{D}(r^*)$.

Indeed, for the choice $r = r^*$ and $D = D^*$, we have

$$G_2(S^{in}, D^*, r^*) = G_{chem}(S^{in}, \overline{D}(1)),$$

509 but D^* is expected to be significantly smaller than $\overline{D}(1)$, the dilution rate that
510 maximises biogas for the simple chemostat. In fact, reducing D means that the
511 flow rate Q has been reduced, and therefore energy has been saved to obtain
512 the same result as with a simple chemostat

513 This result has an important message for practitioners: the serial config-
514 uration is worth considering when mortality is not negligible. To the best of
515 our knowledge, this result is new in the literature. On the other hand, it is not
516 intuitive. For more information on this issue, see Section 5.4. For biological
517 comments on the heuristic underlying this non-intuitive behaviour, the reader
518 is referred to [6].

519 5 Illustrations and numerical simulations

520 This section illustrates of results using three different growth functions. As concave
521 functions, we choose the linear growth function and the Monod function.
522 As a non concave function, we choose the Hill function.

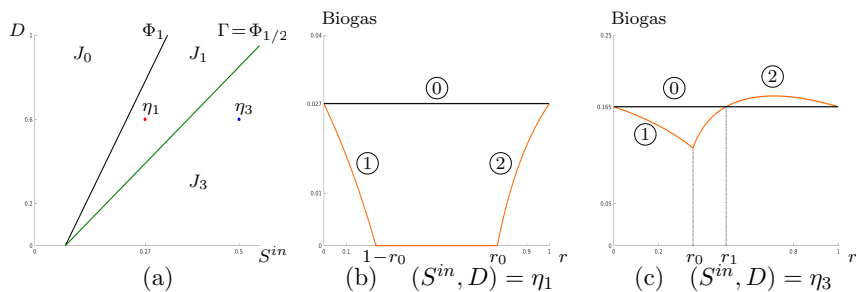


Fig. 7 (a) The regions J_0 , J_1 and J_3 of the operating plane with $f(S) = 4S$ and $a = 0.3$. The biogas flow rates corresponding to points $\eta_1 = (0.27, 0.6) \in J_1$ and $\eta_3 = (0.5, 0.6) \in J_3$ are depicted in panels (b) and (c) respectively. In these panels, the numbered curves ① (in black), and ② (in orange) are respectively defined by $y = G_{chem}(S^{in}, D)$, $y = G_1(S^{in}, D, r)$ and $y = G_2(S^{in}, D, r)$; $r_0(S^{in}, D) = D/(f(S^{in}) - a)$ and $r_1(S^{in}, D)$ is defined by (20). (b) $r_0 \approx 0.77$. (c) $r_0 \approx 0.35$ and $r_1 = 0.5$.

523 5.1 Linear growth function

524 Let consider a linear function $f(S) = \alpha S$, $\alpha > 0$. As it is concave, according
525 to item *ii* in Remark 1, the linear function verifies Assumptions 2 and 3.
526 Therefore, our results apply for a linear function.

527 One has $\lambda(2D + a) = g(D) = (2D + a)/\alpha$ then, the curves $\Phi_{1/2}$, defined by
528 (13), and Γ , defined by (22), are identical. Consequently, the operating plane

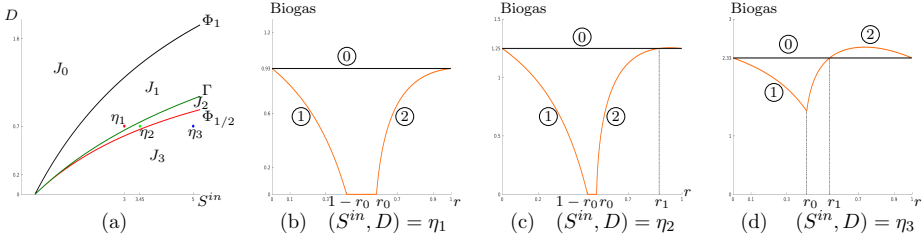


Fig. 8 (a) The regions J_0 , J_1 , J_2 and J_3 in the operating plane with $f(S) = 4S/(5+S)$ and $a = 0.3$. The biogas flow rates corresponding to points $\eta_1 = (3, 0.7) \in J_1$, $\eta_2 = (3.45, 0.7) \in J_2$ and $\eta_3 = (5, 0.7) \in J_3$ are depicted in panels (b), (c) and (d) respectively. In these panels the curves are coloured and numbered as in Fig. 7, $r_0(S^{in}, D) = D/(f(S^{in}) - a)$, and $r_1(S^{in}, D)$ is defined by (20) (b) $r_0 \approx 0.58$. (c) $r_0 \approx 0.53$ and $r_1 \approx 0.87$. (d) $r_0 \approx 0.41$ and $r_1 \approx 0.54$.

529 (S^{in}, D) is divided in three regions J_i , $i = 0, 1, 3$ defined in (23) that describe
 530 the behavior of the output substrate concentration and the biogas flow rate,
 531 see Figure 7(a).

532 Consider the operating points η_1 and η_3 , fixed respectively in regions J_1
 533 and J_3 , as shown in Figure 7(a). The behavior of the biogas flow rate for
 534 these operating points is depicted in Figure 7(b,c). It should be noticed that
 535 for any other point $(S^{in}, D) \in J_1$, the curve representing the biogas flow rate
 536 with respect to r should be similar to the curve shown in Figure 7(a), and
 537 corresponding to $(S^{in}, D) = \eta_1$. Similarly, for any other point $(S^{in}, D) \in J_3$,
 538 it should be similar to the curve shown in Figure 7(b), and corresponding to
 539 $(S^{in}, D) = \eta_3$.

540 In the linear case, the equation $S^{in} = g_r(D)$ is a second degree algebraic
 541 equation in r that gives two solutions, one corresponds to $r_1(S^{in}, D)$ defined
 542 by (20) and the other one is not considered as it does not belong to $(0, 1)$.

543 Since the point $\eta_3 = (0.5, 0.6)$ satisfies the condition $S^{in} > g(D)$, as stated
 544 in item 2 of Proposition 5, the serial configuration has a higher biogas flow
 545 rate production than a single chemostat if and only if $r \in (r_1, 1)$, where
 546 $r_1(0.5, 0.6) \approx 0.5$, see Figure 7 (b).

547 5.2 Monod function

548 The Monod function is $f(S) = mS/(K+S)$. As it is concave, according to item
 549 *ii* in Remark 1, the Monod function verifies Assumptions 2 and 3. Therefore,
 550 our results apply for Monod function.

551 **Lemma 5** For any $D > 0$, the curve Γ , defined by (22), is at left of the curve $\Phi_{1/2}$,
 552 defined by (13).

553 *Proof* The curves $\Phi_{1/2}$ and Γ are respectively defined by equations $S^{in} = \lambda(2D + a)$
 554 and $S^{in} = g(D)$. Let the function $H : [0, (m - a)/2) \mapsto \mathbb{R}$ be defined by

$$H(D) = \lambda(2D + a) - g(D) = \frac{K_m D^2}{(m-D-a)^2(m-a-2D)}.$$

555 Note that $H(0) = 0$ and, for any $D \in (0, (m-a)/2)$, one has $H(D) > 0$ i.e. $\lambda(2D +$
 556 $a) > g(D)$.

557 Hence, the curve Γ is at left of the curve $\Phi_{1/2}$. □

558 As a consequence of Lemma 5, the operating plane (S^{in}, D) is divided in
 559 four regions J_i , $i = 0, 1, 2, 3$ defined in (23) that describe the behavior of the
 560 output substrate concentration and the biogas flow rate, see Fig. 8(a).

561 Consider the operating points η_1, η_2 and η_3 , fixed respectively in regions $J_1,$
 562 J_2 and J_3 , as shown in Fig. 8(a). The behavior of the biogas flow rate for these
 563 points is depicted in Fig. 8(b,c,d). It should be noticed that for any other point
 564 $(S^{in}, D) \in J_1$ (resp. $(S^{in}, D) \in J_2$ and $(S^{in}, D) \in J_3$), the curve representing
 565 the biogas flow rate with respect to r should be similar to the curve shown
 566 in Fig. 8(b) (resp. 8(c) and 8(d)), and corresponding to $(S^{in}, D) = \eta_1$ (resp.
 567 $(S^{in}, D) = \eta_2$ and $(S^{in}, D) = \eta_3$).

568 In the Monod case, the equation $S^{in} = g_r(D)$ is a second degree algebraic
 569 equation in r that gives two solutions, one corresponds to $r_1(S^{in}, D)$ defined
 570 by (20) and the other one is not considered as it does not belong to $(0, 1)$.

571 Since the point η_2 (resp. η_3) satisfies the condition $S^{in} > g(D)$, as stated
 572 in item 2 of Proposition 5, the serial configuration has a higher biogas flow
 573 rate production than a single chemostat if and only if $r \in (r_1, 1)$, with
 574 $r_1(3.45, 0.7) \approx 0.87$ in Fig.8(c) and $r_1(5, 0.7) \approx 0.54$ in Fig. 8(c).

575 5.3 Hill function

576 The Hill function is $f(S) = mS^p/(K^p + S^p)$. Note that if $p = 1$ this function
 577 reduces to the Monod function. For $p > 1$ it is non-concave. We have

$$\lambda(a) = \left(\frac{a}{m-a}\right)^{1/p} K.$$

578 **Proposition 8** *The Hill function satisfies the conditions (34) and (35). Therefore,*
 579 *according to item iii in Remark 1, it verifies Assumption 2 and according to Lemma*
 580 *3, it satisfies Assumption 3.*

581 *Proof* Let us first prove that the Hill function satisfies the condition (35). Straight-
 582 forward computation give

$$\frac{d^2}{dS^2} \left(\frac{1}{f(S)-a} \right) = mpK^p \frac{(p+1)(m-a)S^{2p-2} + (p-1)aK^p S^{p-2}}{((m-a)S^p - aK^p)^3}.$$

583 Therefore, $\frac{d^2}{dS^2} \left(\frac{1}{f(S)-a} \right) > 0$ for all $S > \lambda(a)$, that is to say, (35) is satisfied. This
 584 result can also be obtained without laborious calculations by using item iii of Remark
 585 1. Let $\hat{S} \in (0, +\infty)$ be the inflexion point of the Hill function f . It is sufficient to
 586 show that $(1/f)'' > 0$ for all $S \in (0, \hat{S})$. One easily see that

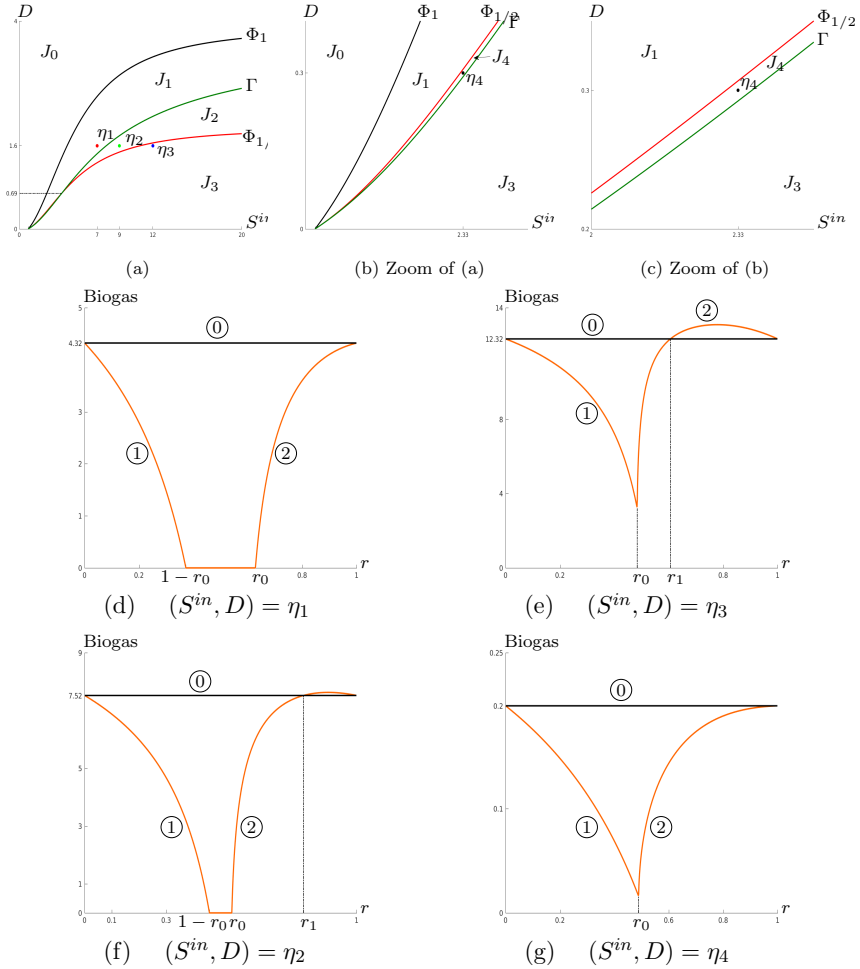


Fig. 9 (a) The regions J_0, J_1, J_2, J_3 and J_4 in the operating plane with $f(S) = 4S^2/(25 + S^2)$ and $a = 0.1$. The curves Γ and $\Phi_{1/2}$ intersects for $D_1 = 0.69$ (see Lemma 6). (b,c) Zooms of (a) showing the region J_4 . The biogas flow rates corresponding to points $\eta_1 = (7, 1.6) \in J_1$, $\eta_2 = (9, 1.6) \in J_2$, $\eta_3 = (12, 1.6) \in J_3$ and $\eta_4 = (2.33, 0.3) \in J_4$ are depicted in panels (d) to (g), respectively. In these panels curves are coloured and numbered as in Fig. 7, $r_0(S^{in}, D) = D/(f(S^{in}) - a)$, and $r_1(S^{in}, D)$ is defined by (20). (d) $r_0 \approx 0.63$. (e) $r_0 \approx 0.54$ and $r_1 \approx 0.81$. (f) $r_0 \approx 0.48$ and $r_1 \approx 0.61$. (g) $r_0 \approx 0.49$.

$$\left(\frac{1}{f}\right)''(S) = \frac{p(p+1)K^p}{mS^{p+2}} > 0,$$

587 for any $S > 0$. Consequently, for all $p > 1$, the Hill function verifies Assumption 2.

588 Let us now prove that the Hill function verifies the condition (34). Straightforward
589 computations give

$$f'(\lambda(D+a)) = \frac{p}{K^p m} (D+a)^{\frac{p-1}{p}} (m-a-D)^{\frac{p+1}{p}}. \quad (44)$$

590 Therefore,

$$f' \left(\lambda \left(\frac{D}{r} + a \right) \right) = \frac{p}{Km} \left(\frac{D}{r} + a \right)^{\frac{p-1}{p}} \left(m - a - \frac{D}{r} \right)^{\frac{p+1}{p}}.$$

591 Since $p > 1$, $D + ra < D + a$ and

$$0 < rm - ra - D < m - a - D,$$

592 one has

$$(D + ra)^{\frac{p-1}{p}} < (D + a)^{\frac{p-1}{p}} \quad (45)$$

$$(rm - ra - D)^{\frac{1}{p}} < (m - a - D)^{\frac{1}{p}}. \quad (46)$$

593 From (45) one has

$$\left(\frac{D}{r} + a \right)^{\frac{p-1}{p}} = \left(\frac{1}{r} \right)^{\frac{p-1}{p}} (D + ra)^{\frac{p-1}{p}} < \left(\frac{1}{r} \right)^{\frac{p-1}{p}} (D + a)^{\frac{p-1}{p}}. \quad (47)$$

594 On the other hand, we have

$$\left(m - a - \frac{D}{r} \right)^{\frac{p+1}{p}} = \left(\frac{1}{r} \right)^{\frac{1}{p}} \left(m - a - \frac{D}{r} \right) A,$$

595 where $A = (rm - ra - D)^{\frac{1}{p}}$. From (46), and using

$$0 < m - a - D/r < m - a - D,$$

596 we then deduce

$$\left(m - a - \frac{D}{r} \right)^{\frac{p+1}{p}} < \left(\frac{1}{r} \right)^{\frac{1}{p}} (m - a - D)^{\frac{p+1}{p}}. \quad (48)$$

597 Therefore, using (44), (47) and (48) one obtains

$$\begin{aligned} f' \left(\lambda \left(\frac{D}{r} + a \right) \right) &= \frac{p}{Km} \left(\frac{D}{r} + a \right)^{\frac{p-1}{p}} \left(m - a - \frac{D}{r} \right)^{\frac{p+1}{p}} \\ &< \frac{p}{Km} \frac{1}{r} (D + a)^{\frac{p-1}{p}} (m - a - D)^{\frac{p+1}{p}} = \frac{1}{r} f'(\lambda(D + a)). \end{aligned}$$

598 This ends the proof of (34). Consequently, according to Lemma 3, any Hill function
599 satisfies Assumption 3. \square

600 Let now consider the case $p = 2$ of the Hill function: $f(S) = mS^2/(K^2 + S^2)$.

601 **Lemma 6** Let $D_1 = (3m - 4a - \sqrt{m(5m - 4a)})/4$. If $0 < D < D_1$ then the curve
602 $\Phi_{1/2}$, defined by (13), at left of the curve Γ , defined by (22). In contrast, if $D_1 <$
603 $D < (m - a)/2$ then the curve $\Phi_{1/2}$ is at right of the curve Γ .

604 *Proof* Let the function $H : [0, (m - a)/2] \mapsto \mathbb{R}$ be defined by $H(D) := \lambda(2D + a) -$
605 $g(D)$. We have

$$H(D) = K \left(\sqrt{\frac{2D+a}{m-a-D}} - \frac{(2D+a)(m-a-D) + (D+a)(m-a)}{2(m-a-D)^{3/2} \sqrt{D+a}} \right).$$

606 Straightforward computation shows that this function is positive if and only if the
607 polynomial

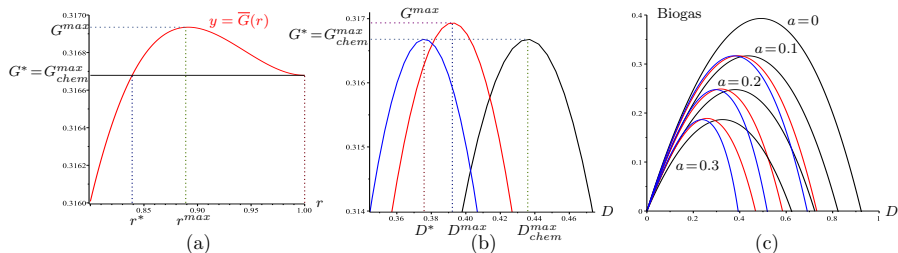


Fig. 10 (a) The map $r \mapsto \overline{G}(r)$ defined by (42), with $f(S) = 4S/(5+S)$, $a = 0.1$ and $S^{in} = 1.5$, showing the values r^* and r^{max} . (b) The corresponding maps $D \mapsto G_{chem}(S^{in}, D)$, in black, $D \mapsto G_2(S^{in}, D, r^*)$, in blue and $D \mapsto G_2(S^{in}, D, r^{max})$, in red, showing the values $D^* < D^{max} < D_{chem}^{max}$. (c) The biogas flow rates for $a = 0, 0.1, 0.2, 0.3$ showing the effects of mortality.

$$Q(D) := 4D^2 - 2(3m - 4a)D + 4a^2 - 5am + m^2$$

608 is negative. The solution of equation $Q(D) = 0$ are

$$D_1 = \frac{3m-4a-\sqrt{\Delta}}{4} \text{ and } D_2 = \frac{3m-4a+\sqrt{\Delta}}{4},$$

609 where $\Delta = 4m(5m - 4a) > 0$, as $a < m$. Notice that we have $0 < D_1 < (m - a)/2$
 610 and $(m - a)/2 < D_2$. Thus, for any $D \in (D_1, (m - a)/2)$, we have $H(D) > 0$ and
 611 then the curve $\Phi_{1/2}$ at right of the curve Γ . \square

612 As a consequence of Lemma 6, the operating plane is divided in five regions
 613 J_i $i = 0, 1, 2, 3, 4$ defined in (23), see Figure 9(a,b,c).

614 Consider the operating points η_1, η_2, η_3 and η_4 fixed respectively in regions
 615 J_1, J_2, J_3 and J_4 , as shown in Figure 9(a,b,c). It should be noticed that
 616 for any other point $(S^{in}, D) \in J_1$ (resp. $(S^{in}, D) \in J_2, (S^{in}, D) \in J_3$ and
 617 $(S^{in}, D) \in J_4$), the curve representing the biogas flow rate with respect to
 618 r should be similar to the curve shown in Fig. 9(a) (resp. (b), (c) and (d)),
 619 and corresponding to $(S^{in}, D) = \eta_1$ (resp. $(S^{in}, D) = \eta_2, (S^{in}, D) = \eta_3$ and
 620 $(S^{in}, D) = \eta_4$).

621 Recall that $r_1(S^{in}, D)$ is defined by (20). It is obtained by solving numerically
 622 the equation $S^{in} = g_r(D)$. Since the point η_2 (resp. η_3) satisfies the
 623 condition $S^{in} > g(D)$, as stated in item 2 of Proposition 5, the serial configura-
 624 tion has a higher biogas flow rate production than a single chemostat if and
 625 only if $r \in (r_1, 1)$, with $r_1(9, 1.6) \approx 0.81$ in Fig. 9(e) and $r_1(12, 1.6) \approx 0.61$, in
 626 Fig. 9(f).

627 5.4 The serial configuration is worth considering when 628 mortality is not negligible

629 In this section we numerically illustrate Remark 2. We fix S^{in} and we adopt
 630 the following notations.

$$D_{chem}^{max} = \overline{D}(1), \quad G_{chem}^{max} = \overline{G}(1) = G_{chem}(S^{in}, D_{chem}^{max})$$

631 where $\overline{G}(r)$ is defined by (42) and $\overline{D}(r)$ is as in Lemma 4. Recall that $r^* \in (0, 1)$
 632 satisfies

$$\overline{G}(r^*) = \overline{G}(1) = G_{chem}^{max}, \quad (49)$$

633 and $\overline{G}(r) > \overline{G}(1)$ for $r \in (r^*, 1)$, so that $\overline{G}(r)$ attains its maximum for $r =$
 634 $r^{max} \in (r^*, 1)$, see Fig. 10(a), obtained with a Monod function and $S^{in} = 1.5$.
 635 We adopt the following notations.

$$D^{max} = \overline{D}(r^{max}), \quad G^{max} = G_2(S^{in}, D^{max}, r^{max})$$

$$D^* = \overline{D}(r^*), \quad G^* = G_2(S^{in}, D^*, r^*) = G_{chem}^{max}$$

Table 1 Numerical values

	$a = 0$	$a = 0.1$	$a = 0.2$	$a = 0.3$
D_{chem}^{max}	0.4918	0.4359	0.3806	0.3259
$G^* = G_{chem}^{max}$	0.3930	0.3167	0.2478	0.1866
r^*	1	0.839	0.717	0.631
D^*	0.4918	0.3758	0.2969	0.2369
r^{max}	1	0.889	0.808	0.751
D^{max}	0.4918	0.3925	0.3190	0.2591
G^{max}	0.3930	0.3169	0.2490	0.1890
$\frac{G^{max} - G_{chem}^{max}}{G_{chem}^{max}}$	0	0.06%	0.5%	1.3%
$\frac{D_{chem}^{max} - D^{max}}{D_{chem}^{max}}$	0	10%	16.2%	20.5%
$\frac{D_{chem}^{max} - D^*}{D_{chem}^{max}}$	0	13.6%	22%	27.3%

636 These notations are illustrated in Figs. 10(a,b). The zoom in Fig. 10(b)
 637 shows that G^{max} exceeds $G^* = G_{chem}^{max}$ only slightly, but D^* is significantly
 638 smaller than D^{max} , which is itself smaller than D_{chem}^{max} . We give in Table 1 the
 639 numerical values of r^* , r^{max} , D^* , D^{max} , G^{max} and $G^* = G_{chem}^{max}$, for various
 640 values of the mortality rate a . The table also gives the relative gains

$$\frac{G^{max} - G_{chem}^{max}}{G_{chem}^{max}}, \quad \frac{D_{chem}^{max} - D^{max}}{D_{chem}^{max}}, \quad \frac{D_{chem}^{max} - D^*}{D_{chem}^{max}},$$

641 when replacing the single chemostat with the serial device using the ratios r^*
 642 and r^{max} . The gain in biogas production is almost negligible, but the gain in
 643 bioreactor flow rate is significant.

644 The biogas flow rates $G_{chem}(S^{in}, D)$, $G_2(S^{in}, D, r^*)$ and $G_2(S^{in}, D, r^{max})$,
 645 for the various considered values of the mortality rate a , are depicted in Fig.
 646 10(c), in black, blue and red, respectively. This figure shows that mortality is
 647 a real problem as it considerably reduces biogas production. Where mortality
 648 cannot be avoided or reduced, instead of using the single chemostat, by using
 649 a serial device, biogas production can be slightly improved while significantly
 650 reducing the bioreactor flow rate.

6 Conclusion

In this work, an in-depth study is carried out on the mathematical model of two interconnected chemostats in serial with mortality. Equations contain a term representing the mortality rate of the species. Due to this added term characterizing the mathematical model, this paper is considered as an extension of the work done in [7], where the model does not consider the mortality rate. However, the mathematical analysis revealed that the proofs have had to be significantly revisited and reveal several new non intuitive differences compared to the case without mortality. Let us recall that without mortality, the dynamics admits a forward attractive invariant hyperplane related to the total mass conservation, which is no longer verified under mortality consideration. This at the core of the differences in the mathematical analysis. The study of the model is based on the analysis of the asymptotic behavior of its solutions, and is supported by an operating diagram which describes the number and stability of steady states. In a first step, we considered different mortality rates a_1 , a_2 in each tank. Then, in view of comparing with the single configuration, we considered identical mortality rate $a = a_1 = a_2$. We analyzed the performances of the model at steady state for two different criteria: the output substrate concentration and the biogas flow rate (and compared them for the single chemostat with the same mortality rate a). Explicit expressions of criteria, depending on the dilution rate D and the input substrate concentration S^{in} , are provided. These new results provide conditions that insure the existence of a serial configuration more efficient than a single chemostat, in the sense of minimizing the output substrate concentration or maximizing the biogas flow rate.

Along the paper, the similarities, specificities and differences of our model compared to the model without mortality (i.e. for $a = 0$) studied in [7] are highlighted. Among the differences that attract attention, on the one hand, we have the operating diagram with different mortality which presents many more cases than the diagram without mortality where it is reduced to only two cases. Thus, the presence of the four regions of stability on the same diagram is now possible. On the other hand, we have the biogas production of the serial device in its maximum state which can be significantly larger than the largest biogas production of the single chemostat. This never happens in the case without mortality. Finally, unlike the case without mortality, the biomass productivity and the biogas flow rate at steady state are not given by the same formulas. Therefore, if biomass productivity is taken into account as a performance criterion, the comparison between the serial chemostat and the single chemostat does not lead to the same conclusions. For more details on this issue the reader can refer to [8].

Appendix A The single chemostat

In this section, we give a brief presentation of the mathematical model of the single chemostat with mortality rate. The mathematical equations are given by

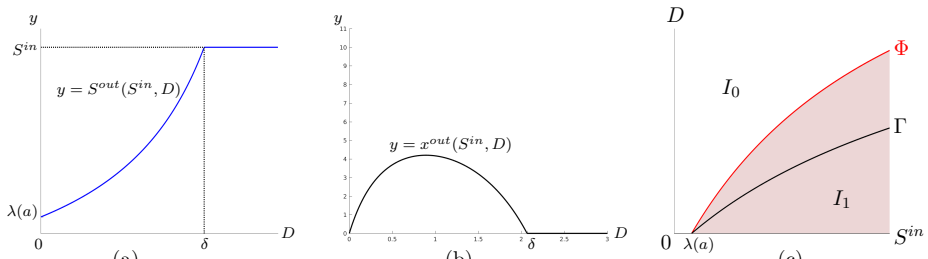


Fig. A1 (a) The map $D \mapsto S^{out}(S^{in}, D)$ is increasing on $[0, \delta]$, where $\delta = f(S^{in}) - a$. (b) The map $D \mapsto x^{out}(S^{in}, D)$ with $f(S) = 4S/(5 + S)$, $S^{in} = 10$ and $a = 0.6$. (c) The curve Γ in the operating plane (S^{in}, D) of the single chemostat.

$$\begin{aligned} \dot{S} &= D(S^{in} - S) - f(S)x, \\ \dot{x} &= -Dx + f(S)x - ax, \end{aligned} \quad (\text{A1})$$

694 where S and x denote respectively the substrate and the biomass concentra-
 695 tion, S^{in} the input substrate concentration, a the mortality rate and $D = Q/V$
 696 the dilution rate, with Q the input flow rate and V the volume of the tank.
 697 The specific growth rate f of the microorganisms satisfies Assumption 1. It is
 698 well known (see [16, 39]) that, besides the washout $F_0 = (S^{in}, 0)$, this system
 699 can have a positive steady state

$$F_1 = (S^*(D), x^*(S^{in}, D)),$$

700 where

$$S^* = \lambda(D + a) \quad \text{and} \quad x^* = \frac{D}{D+a}(S^{in} - \lambda(D + a)).$$

701 See Fig. A1(a) for the plot of the function $D \mapsto S^*(D)$ and Fig. A1(b) for the
 702 plot of the function $D \mapsto x^*(S^{in}, D)$ for $0 \leq D \leq \delta$, where $\delta = f(S^{in}) - a$.

703 The washout steady state F_0 always exists. It is GAS if and only if $D \geq \delta$.
 704 It is LES if and only if $D > \delta$. The positive steady state F_1 exists if and only if
 705 $D < \delta$. It is GAS and LES whenever it exists. Therefore, the curve Φ defined
 706 by

$$\Phi := \{(S^{in}, D) : D = f(S^{in}) - a\} \quad (\text{A2})$$

707 splits the set of operating parameters (S^{in}, D) into two regions, denoted I_0
 708 and I_1 , as depicted in A1(c). These regions are defined by

$$\begin{aligned} I_0 &:= \{(S^{in}, D) : D \geq f(S^{in}) - a\}, \\ I_1 &:= \{(S^{in}, D) : D < f(S^{in}) - a\}. \end{aligned} \quad (\text{A3})$$

709 The behavior of the system in each region is given in Table A1. Figure A1(c),
 710 together with A1 is called the operating diagram of the single chemostat.

711 The particularity of this operating diagram is that the curve limiting both
 712 regions I_0 and I_1 is translated from zero, unlike the case with mortality, as
 713 shown in Figure 2.5 of [16]. Thus, with presence of mortality rate, the region
 714 where the washout is GAS, is larger.

Table A1 Stability of steady states in the various regions of the operating diagram.

	I_0	I_1
F_0	GAS	U
F_1		GAS

715 The output substrate concentration of the single chemostat, at its stable
716 steady state is given by

$$S^{out}(S^{in}, D) = \begin{cases} S^{in} & \text{if } D \geq \delta \\ \lambda(D + a) & \text{if } D < \delta. \end{cases} \quad (\text{A4})$$

717 Its output biomass concentration at steady state is then given by

$$x^{out}(S^{in}, D) = \frac{D}{D+a}(S^{in} - S^{out}(D, a)) \quad (\text{A5})$$

718 For all $S^{in} > \lambda(a)$, one has

$$\frac{\partial S^{out}}{\partial D}(S^{in}, D) = \begin{cases} 0 & \text{if } D > \delta \\ \lambda'(D + a) & \text{if } D < \delta, \end{cases}$$

719 Thus, for any growth function satisfying Assumption 1 the function $D \mapsto$
720 $S^{out}(S^{in}, D)$ is increasing on $[0, \delta]$, as shown in Figure A1(a). The function
721 $D \mapsto x^{out}(S^{in}, D)$ is illustrated in Figure A1(b) for a Monod function.

722 The biogas flow rate of the single chemostat is defined, up to a multiplica-
723 tive yield coefficient, by

$$G_{chem}(S^{in}, D) := Vx^{out}f(S^{out}). \quad (\text{A6})$$

724 Using the expressions (A4) and (A5) respectively of S^{out} and x^{out} , the biogas
725 flow rate of the single chemostat is given by:

$$G_{chem}(S^{in}, D) = \begin{cases} 0 & \text{if } D \geq \delta \\ VD(S^{in} - \lambda(D + a)) & \text{if } D < \delta. \end{cases} \quad (\text{A7})$$

726 For a given $S^{in} > \lambda(a)$, the function $D \mapsto G_{chem}(S^{in}, D)$ is null for $D = 0$ or
727 $D \geq \delta$, and is positive for $D \in (0, \delta)$. Therefore it admits a maximum in $(0, \delta)$,
728 which is assumed to be unique. A characterization of the growth functions for
729 which this uniqueness is satisfied can be found in [31].

730 **Proposition 9** Assume that for any $S^{in} > \lambda(a)$, the maximum of $D \mapsto$
731 $G_{chem}(S^{in}, D)$ is unique, and define $\bar{D}(S^{in}) \in (0, \delta)$, such that

$$G_{chem}(S^{in}, \bar{D}(S^{in})) = \max_{D \geq 0} G_{chem}(S^{in}, D).$$

732 Then, the dilution rate $D = \bar{D}(S^{in})$ is the solution of the equation $S^{in} = g(D)$,
733 where the function $g : [0, m - a] \mapsto \mathbb{R}$ is given by

$$g(D) := \lambda(D + a) + D\lambda'(D + a). \quad (\text{A8})$$

735 *Proof* For any $S^{in} > \lambda(a)$ and $D \in (0, \delta)$, we have

$$\frac{\partial G_{chem}}{\partial D}(S^{in}, D) = V \left(S^{in} - \lambda(D+a) - D\lambda'(D+a) \right) \quad (\text{A9})$$

736 Therefore, $\frac{\partial G_{chem}}{\partial D}(S^{in}, D) = 0$ if and only if $S^{in} = g(D)$, where g is defined by
737 (A8). \square

738 Notice that the function g defined by (A8) is the same as the function
739 g , defined by (19), which was obtained as the limit, when r tends to 1, to
740 the function g_r , defined by (9). Recall that Γ is the curve of equation $S^{in} =$
741 $g(D)$, see (22). This curve is depicted in Fig. A1(c). It is the set of operating
742 conditions given the higher biogas of the single chemostat. More precisely, for
743 any $S^{in} > \lambda(a)$, the maximum $D = \bar{D}(S^{in})$ of the biogas satisfies the condition
744 $(S^{in}, D) \in \Gamma$. Therefore, a sufficient condition for the uniqueness of $\bar{D}(S^{in})$ is
745 that the mapping g is increasing. If, in addition, f is \mathcal{C}^2 , then, deriving (A9)
746 with respect of D , we have

$$\frac{\partial^2 G_{chem}}{\partial D^2}(S^{in}, D) = -Vg'(D).$$

747 Hence, a sufficient condition for Assumption 4 to be satisfied is that $g'(D) >$
748 0 for $D \in [0, m-a)$. This last condition is satisfied whenever $f'' \leq 0$ on
749 $(\lambda(a), +\infty)$, or $\left(\frac{1}{f-a}\right)'' > 0$ on $(\lambda(a), +\infty)$, see Lemma 1 in [31]. Therefore we
750 can make the following remark.

751 *Remark 3* Linear and Monod growth functions satisfy Assumption 4, since they
752 satisfy $f'' \leq 0$ on $(0, +\infty)$. On the other hand the Hill function satisfy Assumption
753 4, since it satisfies $\left(\frac{1}{f-a}\right)'' > 0$ on $(\lambda(a), +\infty)$, as shown in Proposition 8.

754 Appendix B The serial configuration

755 We consider a slight extension of system (1) with different mortality rates in
756 the two tanks. Indeed, we assume that the growth environment differs from
757 one tank to another one. This can lead to two different mortality rates in the
758 tanks. We denote by a_1 and a_2 the mortality rates. The mathematical model
759 is given by the following equations.

$$\begin{aligned} \dot{S}_1 &= \frac{D}{r}(S^{in} - S_1) - f(S_1)x_1 \\ \dot{x}_1 &= -\frac{D}{r}x_1 + f(S_1)x_1 - a_1x_1 \\ \dot{S}_2 &= \frac{D}{1-r}(S_1 - S_2) - f(S_2)x_2 \\ \dot{x}_2 &= \frac{D}{1-r}(x_1 - x_2) + f(S_2)x_2 - a_2x_2. \end{aligned} \quad (\text{B10})$$

760 The following result is classical in the mathematical theory of the chemo-
761 stat.

762 **Lemma 7** For any nonnegative initial condition, the solution of system (B10)
 763 $(S_1(t), x_1(t), S_2(t), x_2(t))$ is nonnegative for any $t > 0$ and positively bounded.

764 *Proof* Since the vector field defined by (B10) is C^1 , the uniqueness of the solution
 765 to an initial value problem holds. From (B10) and using $f(0) = 0$, we have:

$$\begin{aligned} \text{for } i = 1, 2, \quad S_i = 0 &\implies \dot{S}_i > 0, \\ x_1 = 0 &\implies \dot{x}_1 = 0 \\ x_1 \geq 0 \text{ and } x_2 = 0 &\implies \dot{x}_2 \geq 0 \end{aligned}$$

766 Therefore, for $i = 1, 2$, $S_i(t) \geq 0$ and $x_i(t) \geq 0$, for all $t \geq 0$, for which they are
 767 defined, provided $S_i(0) \geq 0$ and $x_i(0) \geq 0$, for $i = 1, 2$, see Prop. B.7 in [39]. This
 768 proves that the solutions of nonnegative initial conditions are always nonnegative.
 769 Let $z_i = S_i + x_i$, $i = 1, 2$. From system (B10), we have

$$z_1 = \frac{D}{r}(S^{in} - z_1) - a_1 x_1, \quad z_2 = \frac{D}{1-r}(z_1 - z_2) - a_2 x_2.$$

770 Consequently, we have the differential inequality

$$z_1 \leq \frac{D}{r}(S^{in} - z_1),$$

771 It follows by comparison of solutions of ordinary differential equations (see for
 772 instance [48]) that one has

$$z_1(t) \leq S^{in} + (z_1(0) - S^{in})e^{-\frac{D}{r}t}$$

773 Therefore, $z_1(t) \leq Z_1$, where $Z_1 = \max(S^{in}, z_1(0))$. Then, we also have the
 774 differential inequality

$$z_2 \leq \frac{D}{1-r}(Z_1 - z_2).$$

775 It follows again by comparison of solutions of ordinary differential equations that one
 776 has also

$$z_2(t) \leq Z_1 + (z_2(0) - Z_1)e^{-\frac{D}{1-r}t}$$

777 Therefore, $z_2(t) \leq Z_2$, where $Z_2 = \max(Z_1, z_2(0))$. Hence, the solutions of (B10) are
 778 positively bounded. Therefore, they are defined for all $t \geq 0$. \square

779 For the description of the steady states, we shall consider the following
 780 function h that will play a key role

$$\begin{aligned} h(S_2) &= \frac{D+(1-r)a_2}{1-r} \frac{S_1^* - S_2}{b - S_2}, \quad S_2 \in (0, b) \\ \text{where } S_1^* &= \lambda \left(\frac{D}{r} + a_1 \right), \quad b = \frac{D(S^{in} - S_1^*)}{D + r a_1} + S_1^*. \end{aligned} \tag{B11}$$

781 This function satisfies the following property.

782 **Lemma 8** Assume that $D/r + a_1 < f(S^{in})$. The function h is decreasing from
 783 $h(0) > 0$ to $h(S_1^*) = 0$, where $h(0)$ is given by

$$h(0) = \frac{D+(1-r)a_2}{1-r} \frac{(D+ra_1)S_1^*}{DS^{in} + ra_1 S_1^*}. \tag{B12}$$

784 *Proof* From the condition $D/r + a_1 < f(S^{in})$ it is deduced that $S_1^* < S^{in}$. Note that

$$b = \frac{DS^{in} + ra_1 S_1^*}{D + ra_1}.$$

785 Hence, b is a convex combination of S^{in} and S_1^* , and we have $S_1^* < b < S^{in}$.
786 Therefore, the vertical asymptote $S_2 = b$ of h is at right of S_1^* . The derivative of h is

$$h'(S_2) = \frac{D + (1-r)a_2}{1-r} \frac{S_1^* - b}{(b - S_2)^2}.$$

787 Hence, we have $h'(S_2) < 0$ for all $S_2 < b$. Therefore, h is defined on the interval
788 $(0, S_1^*)$ and is decreasing from $h(0)$, given by (B12) to $h(S_1^*) = 0$. \square

789 Therefore, if $D/r + a_1 < f(S^{in})$, equation $f(S_2) = h(S_2)$ admits a unique
790 solution, denoted by $S_2^*(S^{in}, D, r)$, as shown in Fig. B2(a). This solution satisfy
791 the following property.

792 **Lemma 9** *Considering $a_1 = a_2 = a$, for all $0 \leq D < f(S^{in}) - a$, one has*

$$\lim_{r \rightarrow 1} S_2^*(S^{in}, D, r) = \lambda(D + a).$$

793

794 *Proof* Let $0 \leq D < f(S^{in}) - a$. Using (5), the condition $h(S_2) = f(S_2)$ is equivalent
795 to

$$\begin{aligned} (D + (1-r)a)(S_1^* - S_2^*) &= \\ (1-r) \left(\frac{D}{D+ra}(S^{in} - S_1^*) + S_1^* - S_2^* \right) f(S_2^*). \end{aligned} \quad (\text{B13})$$

796 For $r = 1$, we have $S_1^* = \lambda(D + a)$. As $\lim_{r \rightarrow 1} f(S_2^*) < +\infty$ then, (B13) gives

$$D(\lambda(D + a) - \lim_{r \rightarrow 1} S_2^*(S^{in}, D, r)) = 0.$$

797 Consequently, one has $\lim_{r \rightarrow 1} S_2^*(S^{in}, D, r) = \lambda(D + a)$. \square

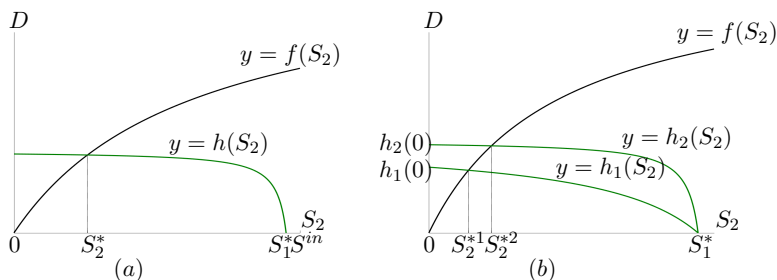


Fig. B2 (a) Existence and uniqueness of the solution S_2^* of equation $f(S_2) = h(S_2)$. (b) Graphical illustration of Proposition 10: S_2^* decreases when S^{in} increases.

798 The existence and stability of steady states of (B10) are given by the
799 following result.

800 **Theorem 3** Assume that Assumption 1 is satisfied. The steady states of (B10) are:

- The washout steady state $E_0 = (S^{in}, 0, S^{in}, 0)$ which always exists. It is GAS if and only if

$$D \geq \max\{r(f(S^{in}) - a_1), (1-r)(f(S^{in}) - a_2)\}. \quad (\text{B14})$$

It is LES if and only if

$$D > \max\{r(f(S^{in}) - a_1), (1-r)(f(S^{in}) - a_2)\}.$$

- The steady state $E_1 = (S^{in}, 0, \bar{S}_2, \bar{x}_2)$ of washout in the first chemostat but not in the second one with

$$\bar{S}_2 = \lambda \left(\frac{D}{1-r} + a_2 \right), \quad \bar{x}_2 = \frac{D}{D+(1-r)a_2} (S^{in} - \bar{S}_2). \quad (\text{B15})$$

It exists if and only if $D < (1-r)(f(S^{in}) - a_2)$. It is GAS if and only if

$$r(f(S^{in}) - a_1) \leq D \text{ and } D < (1-r)(f(S^{in}) - a_2). \quad (\text{B16})$$

It is LES if and only if

$$r(f(S^{in}) - a_1) < D < (1-r)(f(S^{in}) - a_2).$$

- The steady state $E_2 = (S_1^*, x_1^*, S_2^*, x_2^*)$ of persistence of the species in both chemostats with

$$S_1^* = \lambda \left(\frac{D}{r} + a_1 \right), \quad x_1^* = \frac{D}{D+ra_1} (S^{in} - S_1^*), \quad (\text{B17})$$

$$x_2^* = \frac{D}{D+(1-r)a_2} \left(\frac{D}{D+ra_1} (S^{in} - S_1^*) + S_1^* - S_2^* \right) \quad (\text{B18})$$

801 and $S_2^* = S_2^*(S^{in}, D, r)$ is the unique solution of the equation $h(S_2) = f(S_2)$
 802 with h defined by (B11). This steady state exists and is positive if and only
 803 if $D < r(f(S^{in}) - a_1)$. It is GAS and LES whenever it exists and is positive.

804 *Proof* The 4-dimensional system of ODEs (B10) has a cascade structure of two planar
 805 systems of ODEs, whose mathematical analysis is easy and well known in the
 806 mathematical theory of the chemostat [16, 39]. Using this cascade structure, the
 807 global behavior of the system is deduced from the global behaviour of planar systems
 808 and Thieme's theory of asymptotically autonomous systems.

809 For the convenience of the reader the details of the proof are given in Appendix
 810 D.1. \square

811 **Proposition 10** The function $S^{in} \mapsto S_2^*(S^{in}, D, r)$ is decreasing.

812 *Proof* D and r are fixed. Let $S^{in,1} > S^{in,2}$ and h_i defined by (B11), with $S^{in} = S^{in,i}$,
 813 $i = 1, 2$. Let S_2^{*i} , the solution of equation $f(S_2) = h_i(S_2)$, $i = 1, 2$. Using Lemma
 814 8, h_i is a decreasing hyperbola from $h_i(0)$ defined by (B12), with $S^{in} = S^{in,i}$, to
 815 $h_i(S_1^*) = 0$. Since $h_1(0) < h_2(0)$, we have $h_1(S_2) < h_2(S_2)$ for all $S_2 \in (0, S_1^*)$.
 816 Therefore, $S_2^{*1} < S_2^{*2}$, see Fig. B2(b). \square

817 This result means that the effluent steady state concentration of substrate
 818 decreases when the influent concentration of substrate increases. This behavior
 819 is very different from the single chemostat, where the effluent steady state
 820 substrate concentration is independent of the influent substrate concentration.

821 Appendix C Operating diagram

822 For the chemostat model, the operating diagram has as coordinates the input
 823 substrate concentration S^{in} and the dilution rate D , and shows how the solu-
 824 tions of the system behave for different values of these two parameters. The
 825 regions constituting the operating diagram correspond to different qualitative
 826 asymptotic behaviors. Indeed, the main interest of an operating diagram is
 827 to highlight the number and stability of the steady states for a given pair of
 828 parameters (S^{in}, D) . The input substrate concentration S^{in} and the dilution
 829 rate D are the usual parameters manipulated by the experimenter of a chemo-
 830 stat. Apart from these parameters, and the parameter r that can be also chosen
 831 by the experimenter but not easily changed as S^{in} and D , all other paramete-
 832 rs have biological meaning and are fitted using experimental data from real
 833 measurements of concentrations of micro-organisms and substrates. Therefore
 834 the operating diagram is a bifurcation diagram, quite useful to understand the
 835 possible behaviors of the solutions of the system from both the mathematical
 836 and biological points of view.

837 Here, we fix $r \in (0, 1)$ and we depict in the plane (S^{in}, D) the regions
 838 in which the solution of system (B10) globally converges towards one of the
 839 steady state E_0 , E_1 or E_2 . From the results given in Theorem 3, it is seen that
 840 these regions are delimited by the curves Φ_r^1 and Φ_{1-r}^2 defined by:

$$\Phi_r^1 := \{(S^{in}, D) \in \mathbb{R}_+^2 : D = r(f(S^{in}) - a_1)\}, \quad (C19)$$

$$\Phi_{1-r}^2 := \{(S^{in}, D) \in \mathbb{R}_+^2 : D = (1-r)(f(S^{in}) - a_2)\}. \quad (C20)$$

841 When $a_1 = a_2 = 0$, as we have shown in [7], these curves meet only at one
 842 point (the origin) and merge when $r = 1/2$. Therefore, in this case the curves
 843 Φ_r^1 and Φ_{1-r}^2 separate the operating plane (S^{in}, D) , in only three regions, see
 844 [7, Figure 5]. This property continue to hold when $a_1 = a_2$, that is to say,
 845 the curves intersect only at $(\lambda(a_1), 0)$ and merge when $r = 1/2$. In this case
 846 the curves Φ_r^1 and Φ_{1-r}^2 separate the operating plane (S^{in}, D) , in only three
 847 regions, see Figure B3 (c) and (d). The novelty when a_1 and a_2 are different
 848 and non null, is that the intersection of the curves Φ_r^1 and Φ_{1-r}^2 can lie outside
 849 the S^{in} axis. Therefore there can be four regions in the operating plane, as
 850 depicted in Figure B3 (a) and (f). For the description of the intersection of

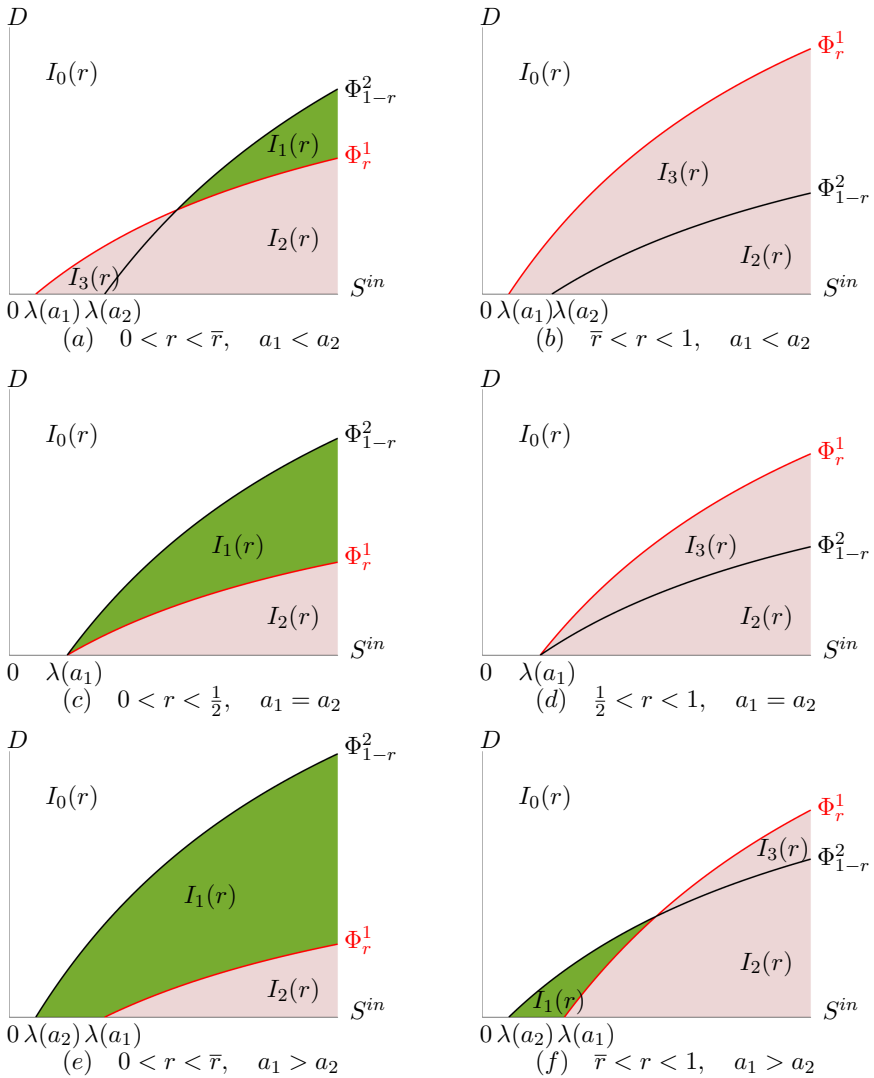


Fig. B3 The operating diagram of (B10). The asymptotic behaviour in each region is depicted in Table C2.

851 the curves Φ_r^1 and Φ_{1-r}^2 , we need some definitions and notations. Let $\bar{r} \in (0, 1)$
 852 be defined by

$$\bar{r} := \frac{m-a_2}{2m-a_1-a_2}. \tag{C21}$$

853 Note that if $a_1 < a_2$ then $\bar{r} < 1/2$, and if $a_1 > a_2$ then $\bar{r} > 1/2$. For $a_1 < a_2$
 854 and $0 < r < \bar{r}$ (or $a_1 > a_2$ and $\bar{r} < r < 1$), we define the point $P = (S_P^{in}, D_P)$
 855 of the operating plane by:

Table C2 The regions $I_k(r)$, $k = 0, 1, 2, 3$ of the operating diagram of (B10) and asymptotic behaviour in these various regions.

Regions
$I_0(r) = \{(S^{in}, D) : \max\{r(f(S^{in}) - a_1), (1-r)(f(S^{in}) - a_2)\} \leq D\}$
$I_1(r) = \{(S^{in}, D) : r(f(S^{in}) - a_1) \leq D \text{ and } D < (1-r)(f(S^{in}) - a_2)\}$,
$I_2(r) = \{(S^{in}, D) : 0 < D < \min\{r(f(S^{in}) - a_1), (1-r)(f(S^{in}) - a_2)\}\}$,
$I_3(r) = \{(S^{in}, D) : (1-r)(f(S^{in}) - a_2) \leq D \text{ and } D < r(f(S^{in}) - a_1)\}$.

	$I_0(r)$	$I_1(r)$	$I_2(r)$	$I_3(r)$
E_0	GAS	U	U	U
E_1		GAS	U	
E_2			GAS	GAS

$$S_P^{in} := \lambda \left(\frac{ra_1 - (1-r)a_2}{2r-1} \right), \quad D_P := \frac{r(1-r)(a_2 - a_1)}{1-2r}. \quad (\text{C22})$$

856 Note that $S_P^{in} > 0$ and $D_P > 0$. With these notations we can state the following
857 result:

- 858 **Proposition 11** 1. If $a_1 < a_2$ then for all $r \in (0, \bar{r})$, the curves Φ_r^1 and Φ_{1-r}^2
859 intersect at the point P and Φ_r^1 is strictly below [resp. above] Φ_{1-r}^2 for
860 $S^{in} > S_P^{in}$ [resp. $S^{in} < S_P^{in}$], see Figure B3 (a). For all $r \in (\bar{r}, 1)$, Φ_r^1 is
861 strictly above Φ_{1-r}^2 , see Figure B3 (b).
- 862 2. If $a_1 > a_2$ then for all $r \in (\bar{r}, 1)$, the curves Φ_r^1 and Φ_{1-r}^2 intersect at the
863 point P and Φ_r^1 is strictly above [resp. below] Φ_{1-r}^2 for $S^{in} > S_P^{in}$ [resp.
864 $S^{in} < S_P^{in}$], see Figure B3 (f). For all $r \in (0, \bar{r})$, Φ_r^1 is below Φ_{1-r}^2 , see
865 Figure B3 (e).
- 866 3. If $a_1 = a_2$ then, for $r = 1/2$, $\Phi_r^1 = \Phi_{1-r}^2$. Moreover, if $r < 1/2$ then Φ_r^1 is
867 strictly below Φ_{1-r}^2 , see Figure B3 (c) and, if $r > 1/2$ then Φ_r^1 is strictly
868 above Φ_{1-r}^2 , see Figure B3 (d).

869 *Proof* For $0 < r < 1$ and $S^{in} > \lambda(a_i)$ we define the function φ_i , $i = 1, 2$, by

$$\begin{aligned} \varphi_1(S^{in}, r) &= r(f(S^{in}) - a_1), \\ \varphi_2(S^{in}, r) &= (1-r)(f(S^{in}) - a_2). \end{aligned} \quad (\text{C23})$$

870 The curves Φ_r^1 and Φ_{1-r}^2 , defined respectively by (C19) and (C20), intersect if and
871 only if there exists $r \in (0, 1)$ and $S^{in} > \max(\lambda(a_1), \lambda(a_2))$ such that $\varphi_1(S^{in}, r) =$
872 $\varphi_2(S^{in}, r)$, that is to say

$$f(S^{in}) = A(r), \quad \text{with} \quad A(r) := \frac{ra_1 - (1-r)a_2}{2r-1}. \quad (\text{C24})$$

873 This equation has a solution $S^{in} > \max(\lambda(a_1), \lambda(a_2))$ if and only if

$$\max(a_1, a_2) < A(r) < m, \quad (\text{C25})$$

874 where $m = \sup(f)$, as in (2). When these conditions are satisfied, the solution of
 875 (C24) is given by $S^{in} = \lambda(A(r))$, where λ is the inverse function of f , i.e. the
 876 break-even concentration defined by (3). Hence, $S^{in} = S_P^{in}$, given in (C22). The
 877 corresponding intersection point of Φ_r^1 and Φ_{1-r}^2 is given by $D_P = r(f(S_P^{in}) - a_1)$,
 878 which is the value given in (C22).

879 Let us determine now for which value of r , the conditions (C25) are satisfied. The
 880 function A is a homographic function. Its graphical representation is a hyperbola,
 881 whose vertical asymptote is $r = 1/2$. Its derivative is given by

$$A'(r) = \frac{a_2 - a_1}{(2r - 1)^2}. \quad (\text{C26})$$

882 Note that $A(r) = m$ if and only if $r = \bar{r}$, where \bar{r} is defined by (C21). Therefore
 883 if $a_1 < a_2$ then, according to (C26), A is increasing. Since $A(0) = a_2$, $A(\bar{r}) = m$,
 884 and $\bar{r} < 1/2$, the condition (C25) is satisfied if and only if $0 < r < \bar{r}$. Similarly, if
 885 $a_1 > a_2$, then, according to (C26), A is decreasing. Since $A(1) = a_1$, $A(\bar{r}) = m$ and
 886 $\bar{r} > 1/2$, the condition (C25) is satisfied if and only if $\bar{r} < r < 1$. Finally, if $a_1 = a_2$
 887 then $A(r) = a_1$ and the condition (C25) cannot be satisfied.

888 Suppose that $a_1 < a_2$. Note that for $0 < r < 1/2$, the condition $f(S^{in}) > A(r)$
 889 [resp. $f(S^{in}) < A(r)$] is equivalent to $\varphi_1(S^{in}, r) < \varphi_2(S^{in}, r)$ [resp. $\varphi_1(S^{in}, r) >$
 890 $\varphi_2(S^{in}, r)$]. Thus:

- 891 • If $r \in (0, \bar{r})$, then $f(S^{in}) < A(r)$ if and only if $S^{in} < S_P^{in}$, where S_P^{in} is defined
 892 by (C22). Hence, the curves Φ_r^1 and Φ_{1-r}^2 intersect at $P = (S_P^{in}, D_P)$ and
 893 the curve Φ_r^1 is strictly below [resp. above] the curve Φ_{1-r}^2 , for all $S^{in} > S_P^{in}$
 894 [resp. $S^{in} < S_P^{in}$].
- 895 • If $r \in [\bar{r}, 1/2)$ then $f(S^{in}) < A(r)$ for all $S^{in} > 0$, so that the curve Φ_r^1 is
 896 strictly above the curve Φ_{1-r}^2 .
- 897 • If $r \in [1/2, 1)$, then, using $r \geq 1 - r$ and $a_1 < a_2$, one has $\varphi_1(S^{in}, r) >$
 898 $\varphi_2(S^{in}, r)$. Therefore, the curve Φ_r^1 is strictly above the curve Φ_{1-r}^2 .

899 If $a_1 > a_2$, the proof is similar to the case $a_1 < a_2$.

900 If $a_1 = a_2$ then $\varphi_1(S^{in}, r) = \varphi_2(S^{in}, r)$ is equivalent to $r(f(S^{in}) - a_1) = (1 -$
 901 $r)(f(S^{in}) - a_1)$. Therefore, $r = 1 - r$, that is $r = 1/2$. In this case the curves Φ_r^1 and
 902 Φ_{1-r}^2 merge. In addition, if $r < 1/2$ [resp. $r > 1/2$] then $r < 1 - r$ [resp. $r > 1 - r$]
 903 and the curve Φ_r^1 is strictly below [resp. above] the curve Φ_{1-r}^2 . This ends the proof
 904 of the proposition. \square

905 For any $r \in (0, 1)$, the curves Φ_r^1 and Φ_{1-r}^2 , defined by (C19) and (C20),
 906 respectively split the plane (S^{in}, D) in the regions denoted $I_0(r)$, $I_1(r)$, $I_2(r)$
 907 and $I_3(r)$ and defined in Table C2. These regions are depicted in Fig. B3 in
 908 the cases $a_1 < a_2$, $a_1 = a_2$ and $a_1 > a_2$.

909 The behavior of the system in each region, when it is not empty, is given in
 910 Table C2. Notice that E_1 exists in both regions $I_1(r)$ and $I_2(r)$, but is stable
 911 only when (S^{in}, D) is fixed in $I_1(r)$.

912 When $a_1 = a_2 = 0$ then $\lambda(a_1) = \lambda(a_2) = 0$ and the curves Φ_r^1 and Φ_{1-r}^2 of
 913 the operating diagram start from the origin of the plane (S^{in}, D) and merge
 914 for $r = 1/2$. Therefore, the diagrams shown in panels (a), (b), (c), (d), (e)
 915 and (f) of Fig. B3 are reduced to only two different cases characterized by
 916 $0 < r < 1/2$ and $1/2 < r < 1$, as shown in Figure 5 of [7]. There is no changes

917 in the stability of the steady states and in the number of the regions depicted
918 in the operating diagram.

919 This result reveals an interplay between spatial heterogeneity (the ratio r of
920 volume distribution between tanks) and the mortality heterogeneity (difference
921 between a_1 and a_2). Indeed, panels (a) and (f) of Fig. B3 bring a particular
922 feature when mortality rates are different: domains $I_1(r)$ and $I_3(r)$ can appear
923 or disappear playing only with the spatial distribution r , a phenomenon which
924 does not happens when mortality is identical in each tank. This shows that
925 the existence of domains $I_1(r)$ and $I_3(r)$ is controlled by a relative toxicity in
926 the tanks, and not only the spatial distribution as it is the case for identical
927 mortality. This feature can have interest when practitioners can adjust pH or
928 other abiotic parameters having impacts on the mortality rate, independently
929 in each tank. Given operating parameters S^{in} , D and r , panels (a) and (f) of
930 Fig. B3 show that it is theoretically possible to pass from domain $I_3(r)$ to $I_2(r)$
931 when mortality parameter is diminished only in the second tank. In practice,
932 being in domain $I_2(r)$ might be more desirable than $I_3(r)$ with respect to some
933 dysfunctioning of the first tank that can drop suddenly its biomass to zero.
934 Indeed, in $I_2(r)$, the second tank is no conducted to the wash-out differently
935 to the $I_3(r)$ case.

936 When $a_1 = a_2 = a$, which is the case corresponding to the system (1)
937 considered in Section 2, only panels (c,d) of Fig. B3 are encountered, as shown
938 in Fig. 2. We describe hereafter the bifurcations that occur in this particular
939 case. The general case i.e. when $a_1 \neq a_2$ is similar.

940 *Remark 4* Transcritical bifurcations occur in the limit cases $D = r(f(S^{in}) - a)$ and
941 $D = (1 - r)(f(S^{in}) - a)$, for system (1). If $0 < r < 1/2$ then, we have a transcritical
942 bifurcation of E_0 and E_1 when $D = (1 - r)(f(S^{in}) - a)$ and a transcritical bifurcation
943 of E_1 and E_2 when $D = r(f(S^{in}) - a)$. If $1/2 < r < 1$ then, we have a transcritical
944 bifurcation of E_0 and E_1 when $D = (1 - r)(f(S^{in}) - a)$ and a transcritical bifurcation
945 of E_0 and E_2 when $D = r(f(S^{in}) - a)$. If $r = 1/2$ and $D = (f(S^{in}) - a)/2$ then, we
946 have transcritical bifurcations of E_0 and E_1 , and E_0 and E_2 , simultaneously.

947 Appendix D Proofs

948 D.1 Proof of Theorem 3

949 We begin by the existence of steady states. The steady states are the solutions
950 of the set of equations $\dot{S}_1 = 0$, $\dot{x}_1 = 0$, $\dot{S}_2 = 0$, $\dot{x}_2 = 0$. From equation $\dot{x}_1 = 0$,
951 it is deduced that $x_1 = 0$ or $f(S_1) = D/r + a_1$. Suppose first that $x_1 = 0$.
952 Then, from equation $\dot{S}_1 = 0$ it is deduced that $S_1 = S^{in}$ and from equation
953 $\dot{x}_2 = 0$ it is deduced that $x_2 = 0$ or $f(S_2) = D/(1 - r) + a_2$. If $x_2 = 0$,
954 then from equation $\dot{S}_2 = 0$ it is deduced that $S_2 = S^{in}$. Hence we obtain the
955 steady state $E_0 = (S^{in}, 0, S^{in}, 0)$, which always exist. On the other hand, if
956 $f(S_2) = D/(1 - r) + a_2$, then $S_2 = \bar{S}_2$, defined in (B15). From equation $\dot{S}_2 = 0$,
957 it is deduced that $x_2 = \bar{x}_2$, defined in (B15). Hence we obtain the steady state

958 $E_1 = (S^{in}, 0, \bar{S}_2, \bar{x}_2)$. This steady state exists if and only if $S^{in} > \bar{S}_2$, that is
 959 $D < (1-r)(f(S^{in}) - a_2)$.

960 Suppose now that $f(S_1) = D/r + a_1$. Then $S_1 = S_1^*$, defined in (B17). From
 961 equation $\dot{S}_1 = 0$, it is deduced that $x_1 = x_1^*$, defined in (B17). From equation
 962 $\dot{S}_2 + \dot{x}_2 = 0$, it is deduced that

$$x_2 = \frac{D}{D + (1-r)a_2}(S_1^* + x_1^* - S_2). \quad (\text{D27})$$

963 Replacing x_2 by this expression in the equation $\dot{S}_2 = 0$, it is deduced that
 964 $f(S_2) = h(S_2)$, where h is defined by (B11). Hence $S_2 = S_2^*$, which is the
 965 unique solution of the equation $f(S_2) = h(S_2)$, as shown in Figure B2 (a).
 966 Replacing S_2 by S_2^* in (D27) gives $x_2 = x_2^*$, defined by (B18). Consequently,
 967 we obtain the steady state $E_2 = (S_1^*, x_1^*, S_2^*, x_2^*)$. This steady state is positive
 968 if and only if $S^{in} > S_1^*$, which is equivalent to $D < r(f(S^{in}) - a_1)$.

969 Let us now study the local stability. Since the system has a cascade struc-
 970 ture, the stability analysis reduces to the study of square 2×2 matrices. Indeed,
 971 the Jacobian matrix associated to system (B10) is the lower triangular matrix
 972 by blocs, $J = \begin{pmatrix} A & 0 \\ B & C \end{pmatrix}$ where B is the diagonal matrix whose diagonal elements
 973 are $D/(1-r)$, and A and C are given by:

$$A = \begin{pmatrix} -\frac{D}{r} - f'(S_1)x_1 & -f(S_1) \\ f'(S_1)x_1 & -\frac{D}{r} + f(S_1) - a_1 \end{pmatrix},$$

$$C = \begin{pmatrix} -\frac{D}{1-r} - f'(S_2)x_2 & -f(S_2) \\ f'(S_2)x_2 & -\frac{D}{1-r} + f(S_2) - a_2 \end{pmatrix},$$

974 Hence, the eigenvalues of J are the ones of A and C .

975 For E_0 , the eigenvalues are $-D/r$, $-D/r + f(S^{in}) - a_1$, $-D/(1-r)$ and
 976 $-D/(1-r) + f(S^{in}) - a_2$. They are negative if and only if $D > r(f(S^{in}) - a_1)$
 977 and $D > (1-r)(f(S^{in}) - a_2)$. Therefore, E_0 is LES if and only if the condition
 978 in the theorem is satisfied.

979 For E_1 , the eigenvalues of A are $-D/r + f(S^{in}) - a_1$ and $-D/r$. The first
 980 eigenvalue is negative if and only if $D > r(f(S^{in}) - a_1)$. On the other hand,
 981 since the determinant of C is positive, and its trace is negative, the eigenvalues
 982 of C are of negative real parts. Therefore, E_1 is LES if and only if the condition
 983 in the theorem is satisfied.

984 For E_2 , the determinant of A is positive and its trace is negative. On the
 985 other hand, using the notation C_{E_2} for the matrix C evaluated at E_2 , we have

$$\det(C_{E_2}) = \left(-\frac{D}{1-r} - f'(S_2^*)x_2^*\right) \left(-\frac{D}{1-r} - a_2 + f(S_2^*)\right) + f(S_2^*)f'(S_2^*)x_2^*,$$

$$\text{tr}(C_{E_2}) = -2\frac{D}{1-r} - a_2 - f'(S_2^*)x_2^* + f(S_2^*).$$

986 Note that $h(S_2) < D/(1-r) + a_2$ for all $S_2 \in (0, S_1^*)$. Therefore, from (B11),
 987 we have $f(S_2^*) = h(S_2^*) < D/(1-r) + a_2$. Consequently, $\det(C_{E_2})$ and $\text{tr}(C_{E_2})$

988 are respectively positive and negative. Therefore, E_2 is LES whenever it exists,
989 that is $D < r(f(S^{in}) - a_1)$.

990 For the study of the global stability we use the cascade structure of the
991 system (B10) and Thieme's Theorem (see Theorem A1.9 of [16]). In the rest of
992 the proof, we denote by $(S_1(t), x_1(t), S_2(t), x_2(t))$ the solution of (B10) with the
993 initial condition $(S_1^0, x_1^0, S_2^0, x_2^0)$. Then, $(S_1(t), x_1(t))$ is the solution of system

$$\begin{aligned}\dot{S}_1 &= \frac{D}{r}(S^{in} - S_1) - f(S_1)x_1 \\ \dot{x}_1 &= -\frac{D}{r}x_1 + f(S_1)x_1 - a_1x_1\end{aligned}\quad (\text{D28})$$

994 with initial condition (S_1^0, x_1^0) and $(S_2(t), x_2(t))$ is the solution of the non-
995 autonomous system of differential equations

$$\begin{aligned}\dot{S}_2 &= \frac{D}{1-r}(S_1(t) - S_2) - f(S_2)x_2 \\ \dot{x}_2 &= \frac{D}{1-r}(x_1(t) - x_2) + f(S_2)x_2 - a_2x_2\end{aligned}\quad (\text{D29})$$

996 with the initial condition (S_2^0, x_2^0) . The system (D28) is the classical model of
997 a single chemostat. Its asymptotic behaviour is well known (see, for instance,
998 Proposition 2.2 of [16]). This system admits the steady states:

$$e_0^1 = (S^{in}, 0) \quad \text{and} \quad e_1^1 = (S_1^*, x_1^*) \quad (\text{D30})$$

999 where S_1^* and x_1^* are defined by (B17). Two cases must be distinguished.

1000 Firstly, if $\lambda(D/r + a_1) \geq S^{in}$, that is $D \geq r(f(S^{in}) - a_1)$ then, e_0^1 , defined
1001 in (D30), is GAS for (D28) in the nonnegative quadrant. Hence, for any non-
1002 negative initial condition (S_1^0, x_1^0) ,

$$\lim_{t \rightarrow +\infty} (S_1(t), x_1(t)) = (S^{in}, 0). \quad (\text{D31})$$

1003 Therefore, the system (D29) is asymptotically autonomous with the limiting
1004 system

$$\begin{aligned}\dot{S}_2 &= \frac{D}{1-r}(S^{in} - S_2) - f(S_2)x_2 \\ \dot{x}_2 &= -\frac{D}{1-r}x_2 + f(S_2)x_2 - a_2x_2.\end{aligned}\quad (\text{D32})$$

1005 Recall that the solutions of (D29) are positively bounded. Therefore, we shall
1006 use Thieme's results which apply for bounded solutions.

1007 The system (D32) represents the classical model of a single chemostat. It
1008 admits the two steady states $e_0^2 = (S^{in}, 0)$ and $e_1^2 = (\bar{S}_2, \bar{x}_2)$, with (\bar{S}_2, \bar{x}_2)
1009 defined by (B15). Two subcases must be distinguished.

- 1010 • If $\lambda(D/(1-r) + a_2) \geq S^{in}$, that is $D \geq (1-r)(f(S^{in}) - a_2)$ then,
1011 e_0^2 is GAS in the nonnegative quadrant. Using Thieme's Theorem, we
1012 deduce that for any nonnegative (S_2^0, x_2^0) , the solution $(S_2(t), x_2(t))$ of
1013 (D29) converges towards $e_0^2 = (S^{in}, 0)$. Using (D31) we deduce that,
1014 when $D \geq \max(r(f(S^{in}) - a_1), (1-r)(f(S^{in}) - a_2))$, the solution
1015 $(S_1(t), x_1(t), S_2(t), x_2(t))$ of (B10) converges towards $E_0 = (S^{in}, 0, S^{in}, 0)$,
1016 which proves (B14).

1017 • In contrast, if $\lambda(D/(1-r) + a_2) < S^{in}$, that is $D < (1-r)(f(S^{in}) - a_2)$
 1018 then, both steady states e_0^2 and e_1^2 exist and e_1^2 is GAS in the positive quad-
 1019 rant. Although system (D29) has the saddle point e_0^2 , no polycycle can exist.
 1020 Using Thieme's Theorem, for any positive (S_2^0, x_2^0) , the solution $(S_2(t), x_2(t))$
 1021 of (D29) converges towards $e_1^2 = (\bar{S}_2, \bar{x}_2)$. Using (D31) we deduce that,
 1022 if $r(f(S^{in}) - a_1) \leq D$ and $D < (1-r)(f(S^{in}) - a_2)$, then the solution
 1023 $(S_1(t), x_1(t), S_2(t), x_2(t))$ of (B10) converges towards $E_1 = (S^{in}, 0, \bar{S}_2, \bar{x}_2)$,
 1024 which proves (B16).

1025 Secondly, if $\lambda(D/r + a_1) < S^{in}$, that is $D < r(f(S^{in}) - a_1)$ then, e_1^1 , defined
 1026 in (D30), is GAS for (D28) in the positive quadrant. Hence, for any positive
 1027 initial condition (S_1^0, x_1^0)

$$\lim_{t \rightarrow +\infty} (S_1(t), x_1(t)) = (S_1^*, x_1^*). \quad (\text{D33})$$

1028 Therefore, the system (D29) is asymptotically autonomous with the limiting
 1029 system

$$\begin{aligned} \dot{S}_2 &= \frac{D}{1-r}(S_1^* - S_2) - f(S_2)x_2 \\ \dot{x}_2 &= \frac{D}{1-r}(x_1^* - x_2) + f(S_2)x_2 - a_2x_2. \end{aligned} \quad (\text{D34})$$

1030 The system (D34) represents the classical model of a single chemostat with an
 1031 input biomass. In this case, there is no washout and the system (D34) always
 1032 admits one LES steady state $e_2 = (S_2^*, x_2^*)$ with positive biomass defined by
 1033 (B18) and S_2^* the unique solution of $h(S_2) = f(S_2)$.

1034 Let us show that this steady state is GAS for (D34). Assume that $x_2 > 0$.
 1035 Consider the change of variable $\xi = \ln(x_2)$. The system (D34) becomes as

$$\begin{aligned} \dot{S}_2 &= \frac{D}{1-r}(S_1^* - S_2) - f(S_2)e^\xi \\ \dot{\xi} &= \frac{D}{1-r}(x_1^*e^{-\xi} - 1) + f(S_2) - a_2. \end{aligned} \quad (\text{D35})$$

The divergence of the vector field

$$\psi(S_2, \xi) = \begin{bmatrix} \frac{D}{1-r}(S_1^* - S_2) - f(S_2)e^\xi \\ \frac{D}{1-r}(x_1^*e^{-\xi} - 1) + f(S_2) - a_2 \end{bmatrix}$$

1036 associated to (D35) is $\text{div}\psi(S_2, \xi) = -\frac{D}{1-r}(1 + x_1^*e^\xi) - f'(S_2)e^\xi$. It is negative.
 1037 Thus, using Bendixon-Dulac criterion, system (D35) cannot have a periodic
 1038 solution. Hence, system (D34) has no cycle in the positive quadrant. For any
 1039 non negative initial condition (S_2^0, x_2^0) , the solution of (D34) is bounded. Hence,
 1040 the ω -limit set of (S_2^0, x_2^0) , denoted $\omega(S_2^0, x_2^0)$, is non-empty and included in the
 1041 positive quadrant. If $e_2 \notin \omega(S_2^0, x_2^0)$ then, using Poincaré-Bendixon Theorem,
 1042 $\omega(S_2^0, x_2^0)$ is a limit cycle, but the system does not present any, due to the
 1043 divergence property. One then deduces $e_2 \in \omega(S_2^0, x_2^0)$ and, as e_2 is LES, then
 1044 $\omega(S_2^0, x_2^0) = \{e_2\}$. Consequently, e_2 is GAS for (D34) in the positive quadrant.
 1045 Using again Thieme's Theorem, for any positive (S_2^0, x_2^0) , the solution
 1046 $(S_2(t), x_2(t))$ of (D29) converges towards $e_2 = (S_2^*, x_2^*)$. Using (D33) we deduce

1047 that, if $D < r(f(S^{in}) - a_1)$, then the solution $(S_1(t), x_1(t), S_2(t), x_2(t))$ of (B10)
 1048 converges towards $E_2 = (S_1^*, x_1^*, S_2^*, x_2^*)$. This ends the proof of the theorem.

1049 D.2 Proof of Lemma 4

1050 Let us fix S^{in} such that $\delta := f(S^{in}) - a > 0$. The proof consists in showing that
 1051 the function $(D, r) \mapsto G_2(S^{in}, D, r)$ can be formally extended as a C^2 function
 1052 for values of r larger than 1 (although such values have no physical meaning).
 1053 Recall first that for any $D \in (0, \delta)$, one has $G_2(S^{in}, D, 1) = G_{chem}(S^{in}, D)$. As
 1054 $G_2(S^{in}, \overline{D}(1), 1) > 0$ and $G_2(S^{in}, 0, 1) = 0$, there exists by continuity of the
 1055 function G_2 , numbers $\underline{D} \in (0, \overline{D}(1))$, $\underline{r} \in (0, 1)$ such that

$$G_2(S^{in}, D, r) < \max_{d \in (0, r\delta)} G_2(S^{in}, d, r), \quad (D, r) \in [0, \underline{D}] \times [\underline{r}, 1]. \quad (D36)$$

1056 Let $\varepsilon > 0$ be such that

$$D_\varepsilon := \varepsilon \left(a + \max_{s \in [0, S^{in}]} f'(s)(S^{in} - s) \right) < \underline{D} \quad (D37)$$

1057 and consider the domain

$$\mathcal{D}_\varepsilon := \left\{ (D, r); \quad D \in (D_\varepsilon, \delta), \quad r \in \left(\max \left(\underline{r}, \frac{D}{\delta} \right), 1 + \varepsilon \right) \right\}.$$

1058 Note that for any $(D, r) \in \mathcal{D}_\varepsilon$, the number $\lambda(D/r + a) = f^{-1}(D/r + a)$ is well
 1059 defined. Posit the function

$$\begin{aligned} \varphi(S_2, D, r) &= (D + (1 - r)a) (\lambda(D/r + a) - S_2) \\ &\quad - (1 - r)f(S_2) \left(\frac{DS^{in} + ra\lambda(D/r + a)}{D + ra} - S_2 \right), \end{aligned}$$

1060 where $(S_2, D, r) \in (0, S^{in}) \times \mathcal{D}_\varepsilon$. As f is C^2 , φ is C^2 on $(0, S^{in}) \times \mathcal{D}_\varepsilon$.

1061 For $r < 1$ and $(D, r) \in \mathcal{D}_\varepsilon$, one has

$$\varphi(S_2, D, r) = (1 - r) \left(\frac{DS^{in} + ra\lambda(D/r + a)}{D + ra} - S_2 \right) (h(S_2) - f(S_2))$$

1062 where h is the function defined in (5). According to Lemma 8, h is posi-
 1063 tive decreasing on $(0, \lambda(D/r + a))$, and $h - f$ admits an unique zero $S_2^* =$
 1064 $S_2^*(S^{in}, D, r)$ on $(0, \lambda(D/r + a))$. Then, one can write

$$\partial_{S_2} \varphi \Big|_{S_2=S_2^*} = (1 - r) \left(\frac{DS^{in} + ra\lambda(D/r + a)}{D + ra} - S_2 \right) (\partial_{S_2} h - f') \Big|_{S_2=S_2^*} < 0.$$

1065 For $r \in [1, 1 + \varepsilon)$ and $(D, r) \in \mathcal{D}_\varepsilon$, one has

$$\begin{aligned} \partial_{S_2} \varphi = & - (D + (1 - r)a) - (1 - r)f'(S_2) \left(\frac{DS^{in} + ra\lambda(D/r + a)}{D + ra} - S_2 \right) \\ & + (1 - r)f(S_2), \end{aligned}$$

1066 which is negative for any $S_2 \in (0, S^{in})$ thanks to condition (D37). As
 1067 $\varphi(0, D, r) > 0$ and $\varphi(S^{in}, D, r) < 0$, we deduce the existence of a unique
 1068 $S_2^* = S_2^*(S^{in}, D, r)$ in $(0, S^{in})$ such that $\varphi(S_2^*, D, r) = 0$, which also verifies
 1069 $\partial_{S_2} \varphi < 0$ at $S_2 = S_2^*$.

1070 Then, by the Implicit Function Theorem, the function $(D, r) \mapsto$
 1071 $S_2^*(S^{in}, D, r)$ is C^2 on \mathcal{D}_ε . Recall that for $r < 1$ and $D < r\delta$, one has the
 1072 expression $G_2(S^{in}, D, r) = VD(S^{in} - S_2^*(S^{in}, D, r))$ (see Proposition 4). We
 1073 extend now the function $(D, r) \mapsto G_2(S^{in}, D, r)$ with this last C^2 expression
 1074 on \mathcal{D}_ε . As $G_2(S^{in}, D, 1) = G_{chem}(S^{in}, D)$ for any $D \in (0, \delta)$, one deduces,
 1075 by continuity of the partial derivatives of G_2 with respect to D and property
 1076 (D36), the existence of $\mathcal{V}_D, \mathcal{V}_r$ as neighborhoods respectively of $\bar{D}(1)$ and 1
 1077 with $\mathcal{V}_D \times \mathcal{V}_r \subset \mathcal{D}_\varepsilon$ such that for any $r \in \mathcal{V}_r$, the function $D \mapsto G_2(S^{in}, D, r)$
 1078 possesses the following properties

- 1079 1. it is strictly concave on \mathcal{V}_D ,
- 1080 2. it is increasing on $(D_\varepsilon, \bar{D}(1)) \setminus \mathcal{V}_D$ and decreasing on $(\bar{D}(1), r\delta) \setminus \mathcal{V}_D$,
- 1081 3. its maximum over $(0, r\delta)$ is not reached for $D \leq D_\varepsilon$.

1082 We thus deduce that $D \mapsto G_2(S^{in}, D, r)$ admits a unique maximum $\bar{D}(r)$ on
 1083 $(0, r\delta)$, for any $r \in \mathcal{V}_r$.

1084 Finally, for any $r \in \mathcal{V}_r$, $\bar{D}(r)$ is characterized as the zero of the map $D \mapsto$
 1085 $F(D, r)$ where F is the C^1 function

$$F(D, r) := \partial_D G_2(S^{in}, D, r)$$

1086 From property 1. above, one obtains

$$\partial_D F(\bar{D}(r), r) = \partial_{DD}^2 G_2(S^{in}, \bar{D}(r), r) < 0, \quad r \in \mathcal{V}_r$$

1087 and by the Implicit Function Theorem, there exists a neighborhood $\mathcal{V}_1 \subset \mathcal{V}_r$
 1088 of 1 such that \bar{D} is C^1 on \mathcal{V}_1 , which ends the proof of the lemma.

1089 D.3 Proof of Proposition 6

1090 S^{in} being fixed, we shall drop the S^{in} dependency in the expressions of S_i^*, x_i^*
 1091 ($i = 1, 2$) and G_2 . Thus, let us define

$$\begin{aligned} G(D, r) &:= G_2(S^{in}, D, r), \\ F_i(D, r) &:= f(S_i^*(D, r))x_i^*(D, r), \quad i = 1, 2, \end{aligned}$$

1092 as functions of $D \geq 0$ and $r \in \mathcal{V}_1 \cap \{r < 1\}$. Remark from the expression of F_1 ,
 1093 that it is well defined as well as its partial derivatives at $r = 1$. In addition,
 1094 for the limiting case $r = 1$, using Lemma 9, for all $D \geq 0$, one has

$$\begin{aligned} S_2^*(D, 1) &= S_1^*(D, 1) = \lambda(D + a) \\ x_2^*(D, 1) &= x_1^*(D, 1) = \frac{D}{D+a}(S^{in} - \lambda(D + a)). \end{aligned} \quad (\text{D38})$$

1095 Thus, for all $D \geq 0$, one has

$$F_1(D, 1) = F_2(D, 1), \quad (\text{D39})$$

1096 and F_2 is also well defined for $r = 1$. Thus, according to (37), for all $D \geq 0$
1097 and $r \in \mathcal{V}_1 \cap \{r \leq 1\}$, one has

$$G(D, r) = rF_1(D, r) + (1 - r)F_2(D, r),$$

1098 and from Lemma 4, for $r \in \mathcal{V}_1 \cap \{r < 1\}$, one has

$$\bar{G}(r) = G(\bar{D}(r), r), \quad (\text{D40})$$

1099 with \bar{G} defined by (42). For convenience, for a function E of (D, r) that is
1100 differentiable, we shall define the three following functions: $\bar{E}(r) := E(\bar{D}(r), r)$
1101 and

$$\partial_r E(r) := \frac{\partial E}{\partial r}(\bar{D}(r), r), \quad \partial_D E(r) := \frac{\partial E}{\partial D}(\bar{D}(r), r).$$

1102 Therefore, the function \bar{G} writes

$$\bar{G}(r) = r\bar{F}_1(r) + (1 - r)\bar{F}_2(r), \text{ for } r \in \mathcal{V}_1 \cap \{r < 1\}. \quad (\text{D41})$$

1103 As the functions F_i are differentiable and as $\bar{D}(r)$ is a maximizer of $D \mapsto$
1104 $rF_1(D, r) + (1 - r)F_2(D, r)$ on the interior of the interval $[0, f(S^{in}) - a]$, one has

$$r\partial_D F_1(r) + (1 - r)\partial_D F_2(r) = 0, \text{ for } r \in \mathcal{V}_1 \cap \{r < 1\}, \quad (\text{D42})$$

1105 and $\partial_D F_1(1) = 0$. As f is \mathcal{C}^2 and \bar{D} is assumed to be differentiable on $\mathcal{V}_1 \cap \{r <$
1106 $1\}$, \bar{G} is differentiable and from (D41), for all $r \in \mathcal{V}_1 \cap \{r < 1\}$, one has

$$\begin{aligned} \bar{G}'(r) &= \bar{F}_1(r) - \bar{F}_2(r) + r\partial_r F_1(r) + (1 - r)\partial_r F_2(r) \\ &\quad + (r\partial_D F_1(r) + (1 - r)\partial_D F_2(r))\bar{D}'(r), \end{aligned}$$

1107 and with (D42), for all $r \in \mathcal{V}_1 \cap \{r < 1\}$, one has simply

$$\bar{G}'(r) = \bar{F}_1(r) - \bar{F}_2(r) + r\partial_r F_1(r) + (1 - r)\partial_r F_2(r). \quad (\text{D43})$$

1108 Let us now determine the limits of the terms of the right side of this last
1109 equality when r tends to 1. Firstly, according to (D39), one has in particular

$$\bar{F}_1(1) = \bar{F}_2(1). \quad (\text{D44})$$

1110 Secondly, remark that the dynamics of the first tank is parameterized by
1111 the single dilution rate $D_1 = D/r$, the other parameters being fixed (see the
1112 expression (B17)). The function F_1 takes then the form $F_1(D, r) = \tilde{F}_1(D/r)$
1113 where \tilde{F}_1 is a smooth function. Therefore, one has

$$\partial_D F_1(r) = -\frac{r}{D(r)}\partial_r F_1(r). \quad (\text{D45})$$

1114 As $\partial_D F_1(1) = 0$ then one deduces

$$\partial_r F_1(1) = 0. \quad (\text{D46})$$

1115 Finally, from $\dot{S}_2 = 0$, for all $r \in \mathcal{V}_1 \cap \{r < 1\}$, one gets

$$F_2(D, r) = \frac{D}{1-r} (S_1^*(D, r) - S_2^*(D, r)). \quad (\text{D47})$$

1116 Differentiating (D47) with respect to r gives

$$\frac{\partial F_2}{\partial r}(D, r) = \frac{D}{1-r} \left(\frac{\partial S_1^*}{\partial r}(D, r) - \frac{\partial S_2^*}{\partial r}(D, r) \right) + \frac{D}{(1-r)^2} (S_1^*(D, r) - S_2^*(D, r))$$

1117 which can be written equivalently as

$$(1-r) \frac{\partial F_2}{\partial r}(D, r) = D \left(\frac{\partial S_1^*}{\partial r}(D, r) - \frac{\partial S_2^*}{\partial r}(D, r) \right) + F_2(D, r).$$

1118 Thus, for $D = \bar{D}(r)$, one has

$$(1-r) \partial_r F_2(r) = \bar{D}(r) (\partial_r S_1^*(r) - \partial_r S_2^*(r)) + \bar{F}_2(r).$$

1119 Notice that for $D = \bar{D}(r)$, (D47) gives

$$\bar{F}_2(r) = \frac{\bar{D}(r)}{1-r} (\bar{S}_1^*(r) - \bar{S}_2^*(r)), \quad \text{for all } r \in \mathcal{V}_1 \cup \{r < 1\}. \quad (\text{D48})$$

1120 Using L'Hôpital's rule in (D48) when r tends to 1, one gets

$$\bar{F}_2(1) = \lim_{r \rightarrow 1^-} \frac{\bar{D}'(r)(\bar{S}_1^*(r) - \bar{S}_2^*(r)) + \bar{D}(r)(\partial_r S_1^*(r) - \partial_r S_2^*(r))}{-1}$$

1121 and using (D38) and (D44), one obtains

$$\bar{F}_1(1) = \lim_{r \rightarrow 1^-} -\bar{D}(r) (\partial_r S_1^*(r) - \partial_r S_2^*(r)).$$

1122 Consequently, one has

$$\lim_{r \rightarrow 1^-} (1-r) \partial_r F_2(r) = 0. \quad (\text{D49})$$

1123 With (D44), (D46) and (D49), expression (D43) gives the existence of the limit
1124 of \bar{G}' when r tends to 1 with $r < 1$, which is

$$\bar{G}'(1^-) = 0. \quad (\text{D50})$$

1125 Note that $\bar{G}''(1^-)$ exists if and only if $\lim_{r \rightarrow 1^-} \frac{\bar{G}'(r) - \bar{G}'(1)}{r-1}$ exists. Using (D50)
1126 and (D43), one has

$$\frac{\bar{G}'(r) - \bar{G}'(1^-)}{r-1} = -\frac{\bar{G}'(r)}{1-r} = -\frac{\bar{F}_1(r) - \bar{F}_2(r) + r \partial_r F_1(r) + (1-r) \partial_r F_2(r)}{1-r} \quad (\text{D51})$$

1127 On the one hand, using L'Hôpital's rule, one has

$$\lim_{r \rightarrow 1^-} \frac{\overline{F}_1(r) - \overline{F}_2(r)}{1 - r} = \lim_{r \rightarrow 1^-} \frac{\overline{F}'_1(r) - \overline{F}'_2(r)}{-1}.$$

1128 Recall that $\partial_r F_1(1) = 0$ and thus one has $\overline{F}'_1(1) = 0$. Consequently, one has

$$\lim_{r \rightarrow 1^-} \frac{\overline{F}_1(r) - \overline{F}_2(r)}{1 - r} = \lim_{r \rightarrow 1^-} \overline{F}'_2(r) = \lim_{r \rightarrow 1^-} \partial_r F_2(r) + \partial_D F_2(r) \overline{D}'(r). \quad (\text{D52})$$

1129 On the other hand, using (D42) and (D45), one has

$$\frac{r}{1 - r} \partial_r F_1(r) = \frac{\overline{D}(r)}{r} \partial_D F_2(r). \quad (\text{D53})$$

1130 Thus, according to (D51), (D52) and (D53), one gets

$$\lim_{r \rightarrow 1^-} \frac{\overline{G}'(r) - \overline{G}'(1^-)}{r - 1} = \lim_{r \rightarrow 1^-} \quad (\text{D54})$$

1131 Let us show now that the limit of $\partial_D F_2(r)$ is 0 when r tends to 1. One has

$$\frac{\partial F_2}{\partial D} = f'(S_2^*) \frac{\partial S_2^*}{\partial D} x_2^* + f(S_2^*) \frac{\partial x_2^*}{\partial D}.$$

1132 Let use the expression $G(D, r) = D(S^{in} - S_2^*(D, r))$ given by Proposition 4.

1133 As $\overline{D}(r)$ is a maximizer then one has

$$\partial_D G(r) = S^{in} - \overline{S}_2^*(r) - \overline{D}(r) \partial_D S_2^*(r) = 0.$$

1134 Using (D38), one then deduces

$$\partial_D S_2^*(1^-) = \frac{S^{in} - \lambda(\overline{D}(1) + a)}{\overline{D}(1)}.$$

1135 In addition, using expressions (B18) and (D38), one gets

$$\partial_D x_2^*(1^-) = -\frac{\overline{D}(1)}{(\overline{D}(1) + a)^2} (S^{in} - \lambda(\overline{D}(1) + a)),$$

1136 and hence the limit of $\partial_D F_2$ when r tends to 1 exists:

$$\partial_D F_2(1^-) = \frac{S^{in} - \lambda(\overline{D}(1) + a)}{\overline{D}(1) + a} f'(\lambda(\overline{D}(1) + a)) A,$$

1137 where $A = S^{in} - \lambda(\overline{D}(1) + a) - \frac{\overline{D}(1)}{f'(\lambda(\overline{D}(1) + a))}$. Thus, one has

$$\partial_D F_2(1^-) = \frac{S^{in} - \lambda(\overline{D}(1) + a)}{\overline{D}(1) + a} f'(\lambda(\overline{D}(1) + a)) (S^{in} - g(\overline{D}(1))),$$

1138 with g defined by (A8). According to Proposition 9, one has $S^{in} - g(\overline{D}(1)) = 0$.

1139 Consequently, one has $\partial_D F_2(1^-) = 0$.

1140 Finally, it remains to calculate the limit of $\partial_r F_2(r)$ when r tends to 1. One
1141 has

$$\frac{\partial F_2}{\partial r} = f'(S_2^*) \frac{\partial S_2^*}{\partial r} x_2^* + f(S_2^*) \frac{\partial x_2^*}{\partial r}.$$

1142 Let us again use the expression $G(D, r) = D(S^{in} - S_2^*(D, r))$. According to (D41),
1143 one has

$$\bar{G}'(r) = \partial_r G(r) + \partial_D G(r) \bar{D}'(r)$$

1144 where $\partial_D G(r) = 0$. According to (D50), we have $\partial_r G(1^-) = 0$, and thus
1145 $\partial_r S_2^*(1^-) = 0$. Using expression (B18), one gets

$$\partial_r x_2^*(1^-) = -a \bar{D}(1) \frac{S^{in} - \lambda(\bar{D}(1) + a)}{(\bar{D}(1) + a)^2},$$

1146 and then the limit of $\partial_r F_2$ when r tends to 1 exists:

$$\partial_r F_2(1^-) = -a \bar{D}(1) \frac{S^{in} - \lambda(\bar{D}(1) + a)}{\bar{D}(1) + a}.$$

1147 As \bar{D}' is assumed to be bounded on $\mathcal{V}_1 \cup \{r < 1\}$, we thus obtain from
1148 (D54) the existence of $\bar{G}''(1^-)$ with

$$\bar{G}''(1^-) = -2\partial_r F_2(1^-)$$

1149 which is given by expression (43).

1150 Acknowledgements

1151 The authors thank Jérôme Harmand for valuable and fruitful comments.
1152 The authors thank the Euro-Mediterranean research network Treasure (<http://www.inra.fr/treasure>).
1153

1154 Conflict of interest

1155 The authors have no relevant financial or non-financial interests to disclose.

1156 Funding

1157 The authors declare that no funds, grants, or other support were received
1158 during the preparation of this manuscript.

1159 Author Contributions

1160 All authors contributed to the study conception, methodology and mathe-
1161 matical analysis. The first draft of the manuscript was written by Manel
1162 Dali-Youcef. All authors commented on previous versions of the manuscript.
1163 All authors read and approved the final manuscript.

1164 **Data Availability**

1165 Data sharing not applicable to this article as no datasets were generated or
1166 analysed during the current study.

1167 **References**

- 1168 [1] N. Abdellatif, R. Fekih-Salem and T. Sari, Competition for a single
1169 resource and coexistence of several species in the chemostat, *Math. Biosci.*
1170 *Eng.*, 13 (2016), 631–652.
- 1171 [2] B. Bar and T. Sari, The operating diagram for a model of competition
1172 in a chemostat with an external lethal inhibitor, *Discrete & Continuous*
1173 *Dyn. Syst. - B*, 25 (2020), 2093–2120.
- 1174 [3] G. Bastin and D. Dochain, *On-line estimation and adaptive control of*
1175 *bioreactors*: Elsevier, Amsterdam, 1991.
- 1176 [4] A. Bornhöft, R. Hanke-Rauschenbach and K. Sundmacher: steady state
1177 analysis of the anaerobic digestion model no. 1 (adm1). *Nonlinear*
1178 *Dynamics* 73 (2013), 535–549.
- 1179 [5] M. Crespo and A. Rapaport, About the chemostat model with a lateral
1180 diffusive compartment, *Journal of Optimization, Theory and Applica-*
1181 *tions*, Vol. 185 (2020), 597—621.
- 1182 [6] M. Dali-Youcef, J. Harmand, A. Rapaport, T. Sari. Some non-intuitive
1183 properties of serial chemostats with and without mortality. 2021. <https://hal.archives-ouvertes.fr/03404740>
- 1184
- 1185 [7] M. Dali-Youcef, A. Rapaport and T. Sari, Study of performance criteria of
1186 serial configuration of two chemostats, *Math. Biosci. Eng.*, 17(6) (2020),
1187 6278-6309.
- 1188 [8] M. Dali-Youcef and T. Sari. The productivity of two serial chemostats
1189 (2021). <https://hal.inrae.fr/hal-03445797>
- 1190 [9] Y. Daoud, N. Abdellatif, T. Sari and J. Harmand: Steady-state analysis
1191 of a syntrophic model: The effect of a new input substrate concentration.
1192 *Math. Model. Nat. Phenom.* 13 (2018), 31.
- 1193 [10] M. Dellal, M. Lakrib and T. Sari, The operating diagram of a model of
1194 two competitors in a chemostat with an external inhibitor, *Math. Biosci.*,
1195 302 (2018), 27–45.

- 1196 [11] R. Fekih-Salem, Y. Daoud, N. Abdellatif and T. Sari. A mathematical
1197 model of anaerobic digestion with syntrophic relationship, substrate inhi-
1198 bition and distinct removal rates. *SIAM Journal on Applied Dynamical*
1199 *Systems* 20 (2021), 621–1654.
- 1200 [12] R. Fekih-Salem, C. Lobry and T. Sari, A density-dependent model of
1201 competition for one resource in the chemostat, *Math. Biosci.*, 286 (2017),
1202 104–122.
- 1203 [13] S. Fogler: *Elements of Chemical Reaction Engineering*, 4th edition.
1204 Prentice Hall, New-York (2008).
- 1205 [14] C. de Gooijer, W. Bakker, H. Beeftink and J. Tramper, Bioreactors
1206 in series: an overview of design procedures and practical applications.
1207 *Enzyme Microb. Technol.* 18 (1996), 202–219.
- 1208 [15] I. Haidar, A. Rapaport, A. and F. Gérard, Effects of spatial structure and
1209 diffusion on the performances of the chemostat. *Mathematical Bioscience*
1210 and *Engineering.* 8(4) (2011), 953–971.
- 1211 [16] J. Harmand, C. Lobry, A. Rapaport and T. Sari, *The Chemostat: Mathe-*
1212 *matical Theory of Microorganism Cultures*, John Wiley & Sons, Chemical
1213 *Engineering Series*, 2017.
- 1214 [17] J. Harmand, A. Rapaport and A. Trofino, Optimal design of two
1215 interconnected bioreactors—some new results. *AIChE J.* 49(6) (1999),
1216 1433–1450.
- 1217 [18] Z. Khedim, B. Benyahia, B. Cherki, T. Sari and J. Harmand: Effect of
1218 control parameters on biogas production during the anaerobic digestion
1219 of protein-rich substrates. *Applied Mathematical Modelling* 61 (2018),
1220 351–376.
- 1221 [19] C.M. Kung and B.C. Baltzis: The growth of pure and simple micro-
1222 bial competitors in a moving and distributed medium. *Math. Biosci.* 111
1223 (1992), 295–313 .
- 1224 [20] O. Levenspiel, *Chemical reaction engineering*, 3rd edition. Wiley, New York
1225 (1999).
- 1226 [21] B. Li, Global asymptotic behavior of the chemostat : general response
1227 functions and differential removal rates. *SIAM Journal on Applied*
1228 *Mathematics* 59 (1998), 411–4.
- 1229 [22] R. W. Lovitt and J.W.T. Wimpenny, The gradostat: a tool for investi-
1230 gating microbial growth and interactions in solute gradients. *Soc. Gen.*
1231 *Microbial Quart.* 6 (1979), 80 .

- 1232 [23] R. W. Lovitt and J.W.T. Wimpenny, The gradostat: a bidirectional com-
1233 pound chemostat and its applications in microbiological research, *J. Gen.*
1234 *Microbiol.* 127 (1981), 261–268
- 1235 [24] K. Luyben and J. Tramper, Optimal design for continuously stirred tank
1236 reactors in series using Michaelis-Menten kinetics. *Biotechnol. Bioeng.* 24
1237 (1982), 1217–1220.
- 1238 [25] M. Nelson and H. Sidhu, Evaluating the performance of a cascade of two
1239 bioreactors. *Chem. Eng. Sci.* 61 (2006), 3159–3166.
- 1240 [26] S. Pavlou, Computing operating diagrams of bioreactors, *J. Biotechnol.*,
1241 71 (1999), 7–16.
- 1242 [27] M. Polihronakis, L. Petrou and A. Deligiannis, Parameter adaptive con-
1243 trol techniques for anaerobic digesters—real-life experiments, Elsevier,
1244 *Computers & chemical engineering*, 17(12) (1993), 1167-1179.
- 1245 [28] A. Rapaport, I. Haidar and J. Harmand, Global dynamics of the buffered
1246 chemostat for a general class of growth functions, *J. Mathematical*
1247 *Biology*, 71(1) (2015), 69–98.
- 1248 [29] A. Rapaport and J. Harmand, Biological control of the chemostat
1249 with nonmonotonic response and different removal rates. *Mathematical*
1250 *Biosciences and Engineering* 5, no. 3 (2008), 539–547.
- 1251 [30] T. Reh and J. Muller, CO₂ abatement costs of greenhouse gas (GHG)
1252 mitigation by different biogas conversion pathways. *J. Environ. Manag.*
1253 114, no. 15 (2013), 13–25.
- 1254 [31] T. Sari. Best Operating Conditions for Biogas Production in Some Simple
1255 Anaerobic Digestion Models. *Processes* 2022, 10, 258.
- 1256 [32] T. Sari and B. Benyahia. The operating diagram for a two-step anaerobic
1257 digestion model. *Nonlinear Dynamics* 2021, **105**, 2711–2737.
- 1258 [33] T. Sari and J. Harmand, A model of a syntrophic relationship between two
1259 microbial species in a chemostat including maintenance, *Math. Biosci.*,
1260 275 (2016), 1–9.
- 1261 [34] T. Sari and F. Mazenc, Global dynamics of the chemostat with different
1262 removal rates and variable yields. *Math Biosci Eng.* 8(3) (2011), 827–40.
- 1263 [35] T. Sari and M.J. Wade, Generalised approach to modelling a three-tiered
1264 microbial food-web, *Math. Biosci.*, 291 (2017), 21–37.
- 1265 [36] M. Sbarciog, M. Loccufer and E. Noldus, Determination of appropriate
1266 operating strategies for anaerobic digestion systems, *Biochem. Eng. J.*, 51

1267 (2010), 180–188.

1268 [37] H. Smith, The gradostat: A model of competition along a nutrient
1269 gradient. *Microbial Ecology*, 22(1) (1991), 207–26.

1270 [38] H. Smith, B. Tang and P. Waltman: Competition in a n-vessel gradostat.
1271 *SIAM J. Appl. Math.* 91(5) (1991), 1451–1471.

1272 [39] H. Smith and P. Waltman, *The Theory of the Chemostat, Dynamics of*
1273 *Microbial Competition*. Cambridge University Press, 1995.

1274 [40] B. Tang, Mathematical investigations of growth of microorganisms in the
1275 gradostat, *J. Math. Biol.*, 23 (1986), 319–339.

1276 [41] M.J. Wade, R.W. Pattinson, N.G. Parker and J. Dolfing, Emergent
1277 behaviour in a chlorophenol-mineralising three-tiered microbial ‘food
1278 web’, *J. Theor. Biol.*, 389 (2016), 171–186.

1279 [42] M. Weederemann, G. Seo and G.S.K Wolkowics: Mathematical model of
1280 anaerobic digestion in a chemostat: Effects of syntrophy and inhibition.
1281 *Journal of Biological Dynamics* 7 (2013), 59–85.

1282 [43] M. Weederemann, G.S.K Wolkowicz and J. Sasara: Optimal biogas produc-
1283 tion in a model for anaerobic digestion. *Nonlinear Dynamics* 81 (2015),
1284 1097–1112.

1285 [44] G.S.K. Wolkowicz, Z. Lu, Global dynamics of a mathematical model of
1286 competition in the chemostat: general response functions and differential
1287 death rates. *SIAM Journal on Applied Mathematics* 52 (1992), 222–23.

1288 [45] A. Xu, J. Dolfing, T.P. Curtis, G. Montague and E. Martin, Maintenance
1289 affects the stability of a two-tiered microbial ‘food chain’?, *J. Theor. Biol.*,
1290 276 (2011), 35–41.

1291 [46] J. Zambrano and B. Carlsson, Optimizing zone volumes in bioreactors
1292 described by Monod and Contois growth kinetics, *Proceeding of the IWA*
1293 *World Water Congress & Exhibition*, (2014).

1294 [47] J. Zambrano, B. Carlsson and S. Diehl, Optimal steady-state design of
1295 zone volumes of bioreactors with Monod growth kinetics. *Biochem. Eng.*
1296 *J.* 100 (2015), 59–66.

1297 [48] W. Walter, *Ordinary Differential Equations*. Springer Graduate Texts in
1298 *Mathematics*, 182 (1998).